CHAPTER 7 CONDUCTIVITY RESULTS AND DISCUSSION

7-1 Introduction

The main objective of this chapter is to explore the potential conductivity benefits which can be achieved through the use of carbon nanographite, and other related fillers, to improve the performance of thermoplastic toughened composite matrix materials.

7-2 Materials and Experimental Methods

The materials utilised in this chapter have been fully detailed at the start of Chapter 6. Therefore only a brief summary is included at this point.

Polypyrrole was synthesised electrochemically as well as purchased from Aldrich and BASF. Conductivity comparisons and doping were carried out on all samples. The doping of carbon fibre is also considered. The incorporation of nanographite into a thermoplastic matrix is considered; the matrices utilised include a commercial poly(ethersulfone)-based co-polymer (PES), PEEK and PEKK. In addition the incorporation of carbon nanotubes, carbon black (XC605 and XC72), TTF TCNQ (tetrathiafulvelene 7,7,8,8-tetracyanonitroquinodimethane salt) and copper(II) phthalocyanine was also considered.

In addition the effect of processing these materials in an extruder and a Plasti-Corder® is also considered.

7-3 Results and Discussion

7-3-1 Polypyrrole and Carbon Fibre

7-3-1-1 Electrochemically Synthesised Polypyrrole Films

Following the experimental procedure detailed in Section 6-3-1 polypyrrole was manufactured in thin films. A picture of the shavings of such a film is shown in Figure 7-1.

Figure 7-1 – Polypyrrole film shavings

Six films, in total, were grown at potentials ranging from 0.68 V to 0.8 V. The first two films were grown in conditions where only one side of the electrode was coated with a chrome-on-gold layer, therefore only one side of the electrode could be utilised to grow the polymer. The last four films were grown under conditions where both sides of the electrode were coated in gold. In total, therefore, four polymerisations were carried out. When utilising both sides of the electrode to grow the films, one side was situated in front of the cathode – this side is subsequently referred to as side A, the other side is referred to as side B. The thicknesses of the films are shown in Table 7-1.

Table 7-1 – Thickness of synthesised polypyrrole films

Film	1 (0.68V)	2 (0.68V)	3A (0.8 V)	3B (0.8 V)	4A (0.75V)	4B (0.75V)
Thickness / µm	5-10	5-10	40-42	18-22	50-60	18-23

It is seen from Table 7-2 that films polymerised on side B, are significantly less thick than those polymerised on side A. This is undoubtedly due to the positioning of the electrodes to the cathode. The conductivities of these electrochemically-synthesised films were measured, and the results are shown in Table 7-2

Table 7-2– Conductivities of Strathclyde synthesised polypyrrole

Film	1	2	3a	3b	4a	4b
Conductivity / Sm^{-1}	873	914	984	1183	1071	1059

7-3-1-2 Polypyrrole powder purchased from Aldrich

In order to compare the conductivities of the synthesised polypyrrole films to that which can be purchased, polypyrrole powder doped with sulfonic acid was purchased from Aldrich. The powder was pressed into discs using a 13 mm IR disc press, as previously detailed in Section 6-3-2-4. Also discussed in this section is the fact that the conductivity of these polypyrrole discs is given by Equation 6-5. The resultant conductivities are shown in Table 7-3.

Table 7-3 – Conductivities of polypyrrole purchased from Aldrich

Disc	1	2	3	4	5
Conductivity / Sm^{-1}	89	123	77	87	92

It can be seen that the conductivity of the Aldrich purchased polypyrrole is approximately one order of magnitude less than that which was electrochemically synthesised. It can also be seen that there is quite a large degree of intra-sample variation, which is attributed to the experimental technique used to measure the

conductivity. The four-point probe measures the surface conductivity, and is therefore dominated by the compression close to the surface. As the samples are pressed into discs using an IR dye press, the conductivity measured will be affected by the degree of compacting, and more specifically, the position of the nanographite platelets close to the surface.

7-3-1-3 Polypyrrole purchased from BASF

The conductivity of the polypyrrole strips purchased from BASF is shown in Table 7-4. It is seen that, in general, the conductivity is higher than that of the polypyrrole purchased from Aldrich, but not as high as that of the Strathclyde synthesised polypyrrole.

Table 7-4 – Conductivities of polypyrrole bought from BASF

Strip	**1**	**2**	**3**	**4**	**5**
Conductivity / Sm^{-1}	386	411	354	387	456

7-3-1-4 Carbon Fibre

The experimental procedure detailed in Section 6-3-2-5 was followed in order to measure the conductivity of the carbon fibre. The results obtained are shown in Table 7-5.

Table 7-5 – Conductivities of carbon fibre

Carbon Fibre	**1**	**2**	**3**	**4**	**5**
Conductivity / Sm^{-1}	**777**	**696**	**937**	**967**	**832**

It is seen from Table 7-5 that the conductivity of the carbon fibre is higher than that of the purchased polypyrrole, and has a similar conductivity to the Strathclyde synthesised material.

7-3-2 Doping

7-3-2-1 Electrochemically Synthesised Polypyrrole

The conductivity of polypyrrole is closely related to the number of oxidised-quaternised nitrogens. Therefore it is anticipated that treatment with acid (and alkali) should therefore be expected to induce changes in the conductivity. The procedure detailed in Section 6-3-3-1, was followed and Strathclyde synthesised films of polypyrrole were doped in HCl and HNO_3 accordingly. The results are shown in Table 7-6**,** and Figure 7-2. Film 3A which had a conductivity of 984 S/m before doping was exposed to both HCl and HNO_3.

Table 7-6 – Conductivities of synthesised polypyrrole after doping

HCl				
Concentration / M	0	0.6	3	6
Conductivity / Sm^{-1}	984	4853	5292	5438
HNO_3				
Concentration / M	0	0.5	1	2
Conductivity / Sm^{-1}	984	3593	4400	4651

It is noted at this point that the calculations used to determine the errors associated with the conductivity values of all types of polypyrrole are outlined in Appendix 2.

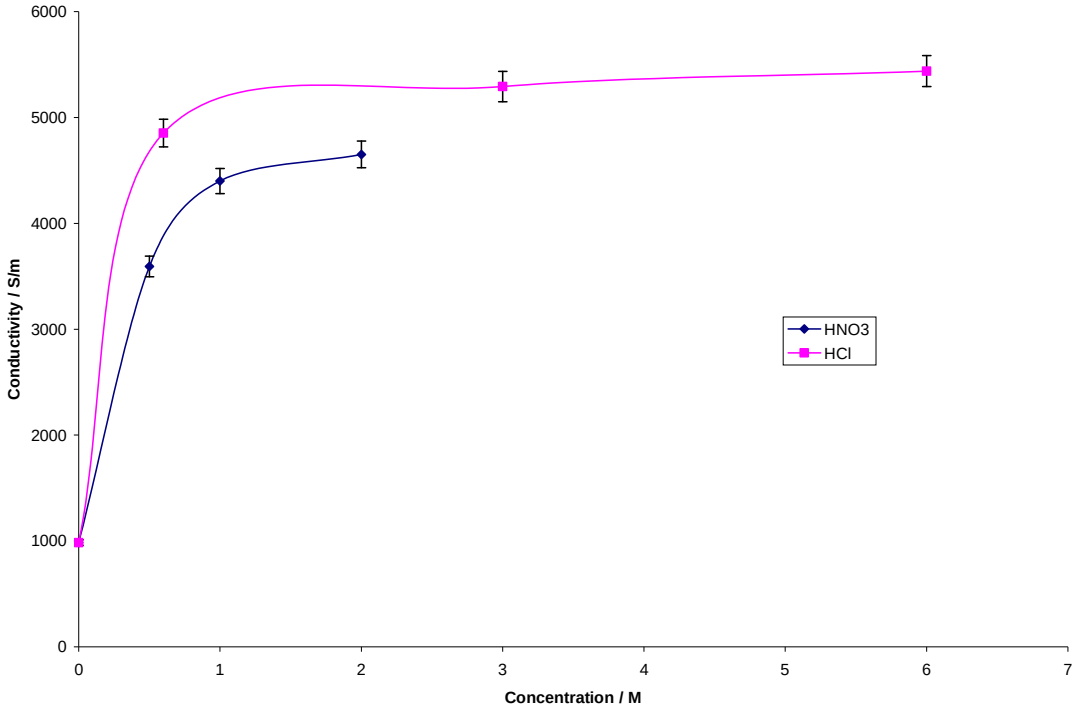

Figure 7-2 – Synthesised polypyrrole film doped in HNO_3 and HCl

It is seen that exposure to acid does indeed increase the conductivity. The highest increase is seen for polypyrrole doped in 6 M HCl. The increased conductivity can be attributed to the generation of free protonic carriers which will be able to migrate through the polymer matrix. In basic conditions the polymer is not quaternised and hence is unable to release free protonic conductors. In this study it is seen that both HCl and HNO_3 increase the conductivity.

7-3-2-2 Polypyrrole Powder Purchased from Aldrich

The conductivities measured when discs of polypyrrole purchased from Aldrich were exposed to HCl and HNO_3 are shown in Table 7-7 and Figure 7-3.

Table 7-7 – Conductivities of polypyrrole discs after doping

HCl				
Concentration (M)	0	0.6	3	6
Conductivity / Sm^{-1}	92	88	84	93
HNO_3				
Concentration (M)	0	0.5	1	2
Conductivity / Sm^{-1}	92	53	55	54

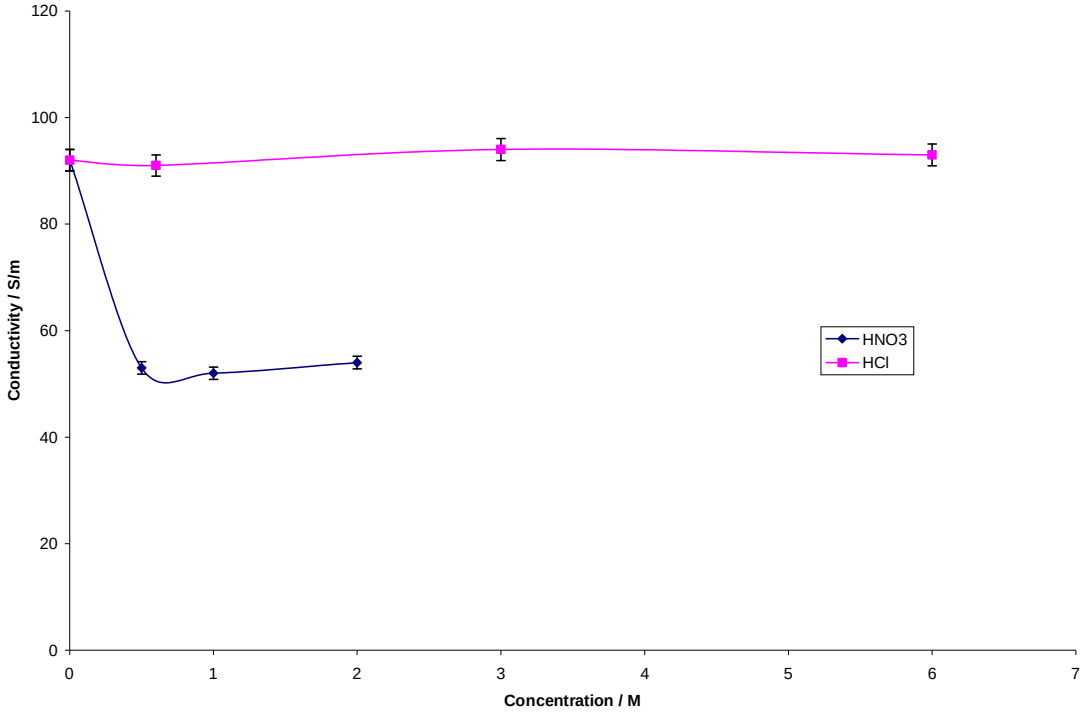

Figure 7-3– Polypyrrole discs doped in HNO_3 and HCl

In this case it is seen that there is very little difference in the conductivities obtained when doped in HCl, and a decrease in the conductivities obtained when doped in HNO_3. This is most probably due to the fact that, when purchased, the polypyrrole was already doped with sulfonic acid, therefore there is no benefit obtained by further doping.

7-3-2-3 Polypyrrole Purchased from BASF

The conductivity results of the BASF purchased polypyrrole, after doping, are shown in Table 7-8, and Figure 7-4.

Table 7-8 – Conductivities of BASF polypyrrole after doping

HCl				
Concentration / M	0	0.6	3	6
Conductivity / Sm^{-1}	386	525	573	587
HNO_3				
Concentration / M	0	0.5	1	2
Conductivity / Sm^{-1}	386	265	153	126

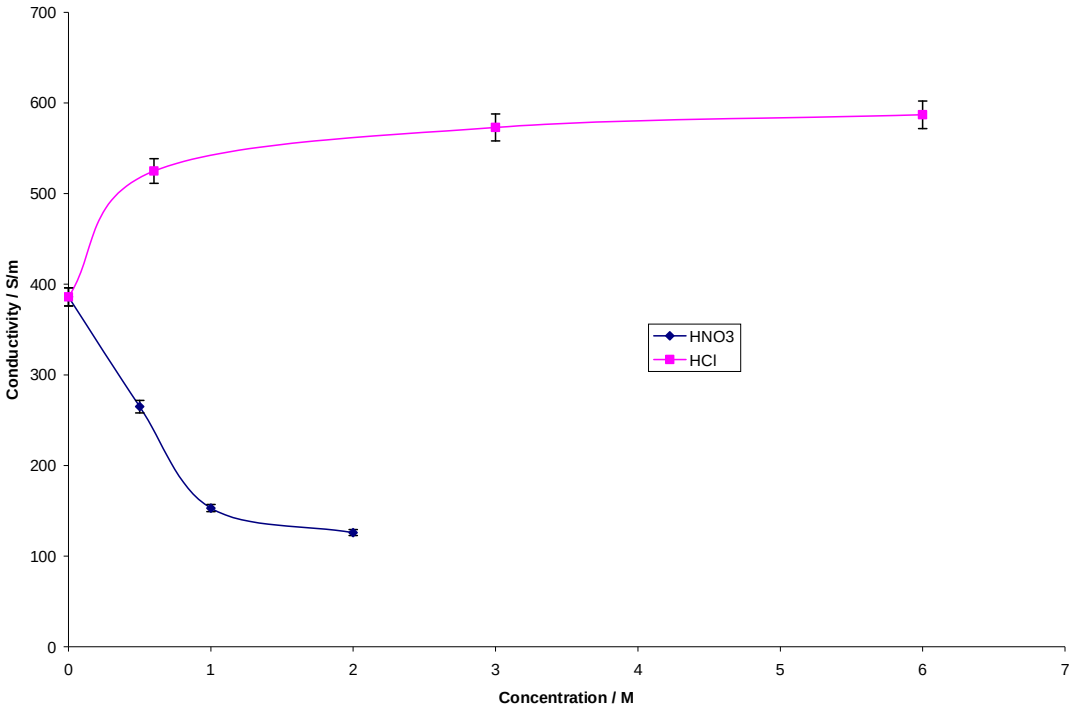

Figure 7-4– Polypyrrole film, supplied by BASF, doped in HNO_3 and HCl

It is again seen that the highest conductivity is obtained for the polypyrrole doped in 6 M HCl, though again, there is not a significant increase in conductivity obtained when using the higher levels of HCl. It is also seen that the lowest conductivity is obtained when the polypyrrole is doped in 2 M HNO_3. When we consider the conductivity of the matrix it must be appreciated that in the presence of a strong acid the nitrogen of the polypyrrole will be quaternized and this in turn will liberate the counter ion, which can then migrate under the influence of the electric field. Thus, the differences between the two acids are attributed to the anion which is generated. The nitrate is a much larger anion than the chloride, and it is possible that it will be less mobile in the matrix than the chloride. The drop in the conductivity with increasing concentration is however rather more difficult to explain and implies that some form of trapping must be occurring.

7-3-2-4 BASF Film Thickness and Mass Before and After Acid Exposure[1]

It is seen, from Table 7-9, that the thickness and mass loss of the BASF polypyrrole after exposure to acid is significant, up to an average of 12.8 % loss in thickness after exposure to 3 M HCl, and up to an average of 24.6 % loss in mass after exposure to 6 M HCl. It has been suggested that the loss is due to ion exchange occurring, with replacement of the large *p*-toluene sulfonate ions with smaller chlorine ions.[1] It is possible that the apparent reduction in conductivity experienced with the inclusion of HNO_3 reflects the effects of ion exchange between the nitrate and the *p*-toluene sulfonate. The conductivity will be determined both by the transport of electronic charge and also ionic charged species. The charge will move between polymer chains by protonic conduction but this must be balanced by the compensating movement of anions, which is reflected in the sensitivity of the conduction to the type of anion present.

Table 7-9- % loss in mass and thickness after BASF polypyrrole exposure to acid

	Average thickness / mm				Average mass / mg			
	Before	**After**	**% Loss**	**Average % loss**	**Before**	**After**	**% Loss**	**Average % loss**
6 M HCl	0.078	0.069	11.5	10.0	15.19	11.59	23.7	24.6
	0.075	0.070	7.1		14.84	11.10	25.2	
	0.078	0.069	11.5		15.26	11.46	24.9	
3 M HCl	0.077	0.068	11.7	12.8	11.44	11.44	24.7	24.1
	0.083	0.070	14.9		11.34	11.34	25.5	
	0.080	0.071	11.6		11.75	11.75	22.1	
1.2 M HCl	0.076	0.070	7.9	9.0	15.15	12.08	20.3	19.7
	0.075	0.067	11.5		14.93	11.86	20.6	
	0.080	0.074	7.5		15.17	12.42	18.1	
0.12 M HCl	0.080	0.073	9.5	7.0	15.68	12.79	18.4	16.5
	0.079	0.074	6.8		15.73	13.05	17.0	
	0.078	0.074	4.7		15.06	12.95	14.0	

7-3-2-5 BASF Polypyrrole Doped with Alkali

From Table 7-10 the results of BASF polypyrrole after exposure to NaOH can be seen; the resulting graph can be seen in Figure 7-5. It is seen that the conductivity is significantly reduced when the polypyrrole is doped in base – being eight orders of magnitude less than when the same material is doped in acid. The conductivity appears to level off at a value of 2.8×10^{-6} Sm^{-1}. It is therefore concluded that the ability of the material to carry charge has been terminated, and the polypyrrole is now behaving as an insulator.

Table 7-10 – Concentration and resultant conductivity values for BASF films doped in NaOH

Concentration / M	Conductivity / Sm^{-1}
0	386
0	386
0	386
0.1	3.98×10^{-6}
0.1	3.88×10^{-6}
0.1	3.39×10^{-6}
0.2	2.76×10^{-6}
0.2	2.54×10^{-6}
0.2	2.73×10^{-6}
1	2.77×10^{-6}
1	2.58×10^{-6}
1	2.81×10^{-6}
2	2.70×10^{-6}
2	2.80×10^{-6}
2	2.92×10^{-6}

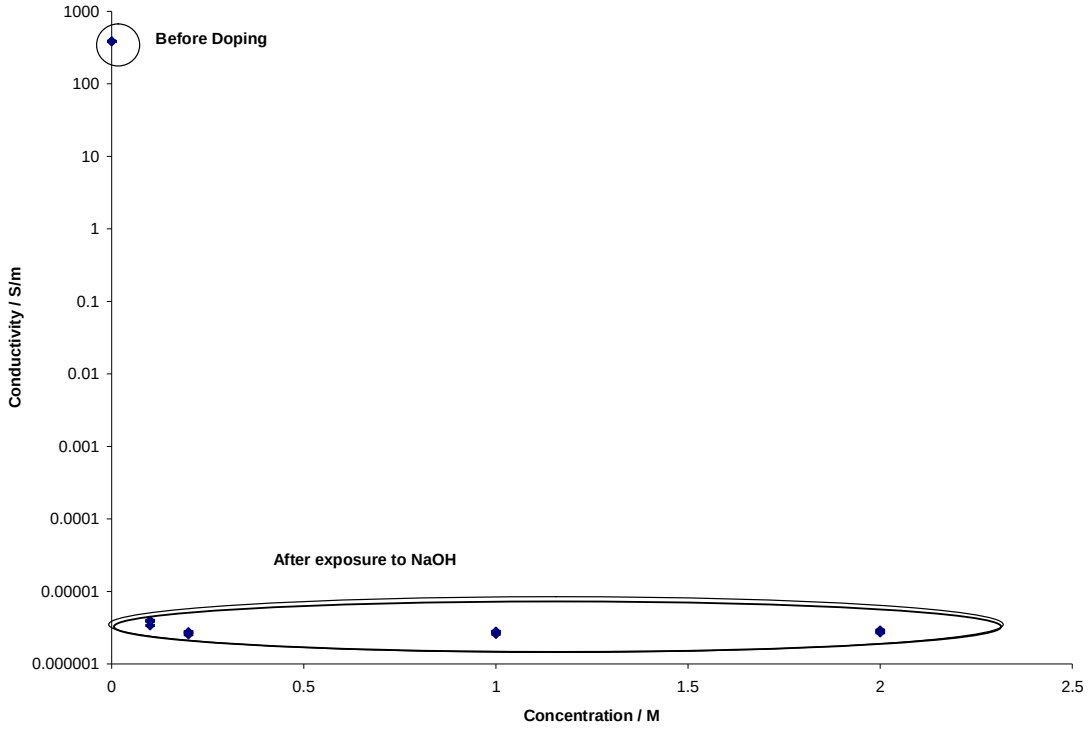

Figure 7-5 – Graph of conductivity vs. base concentration for BASF polypyrrole

As indicated above, treatment with the hydroxide will remove all of the quaternisation, which leads to two effects; it reduces the intrinsic conductivity of the polypyrrole, and reduces the number of free charge carriers which allow hopping between the conducting polymer chains.

7-3-2-6 Carbon Fibre

Table 7-11 and Figure 7-6 show the conductivities obtained after carbon fibres were doped, in triplicate, in HCl and HNO_3. It is interesting to note that, this time, the highest conductivity value, 14,612 S/m, is obtained when the fibre is doped in 3 M HNO_3. When the fibre is doped in 7.5 M HNO_3, the conductivity drops to 4938 S/m.

The worked calculations, and errors, associated with the carbon fibre doping are shown in Appendix 2.

Table 7-11– Conductivity after carbon fibre is doped in acid

	HCl / M				HNO_3 / M			
Acid concentration	0	0.6	3	6	0	0.5	3	7.5
Carbon fibre conductivity / Sm^{-1}	960	3415	5284	2505	960	9002	14612	4938

Although we normally think of carbon fibre as being made up of pseudo aromatic rings, in practice there will often be as much as 5 % nitrogen contained within the structure. Carbon fibre is produced from acrylonitrile, and in the pyrolysis process ammonia is evolved. However this process is not 100 % efficient and there will be a small amount of nitrogen still left in the carbon fibres. This nitrogen can be quaternised in the same manner as in polypyrrrole and hence the same enhancement in conductivity is possible upon acid treatment.

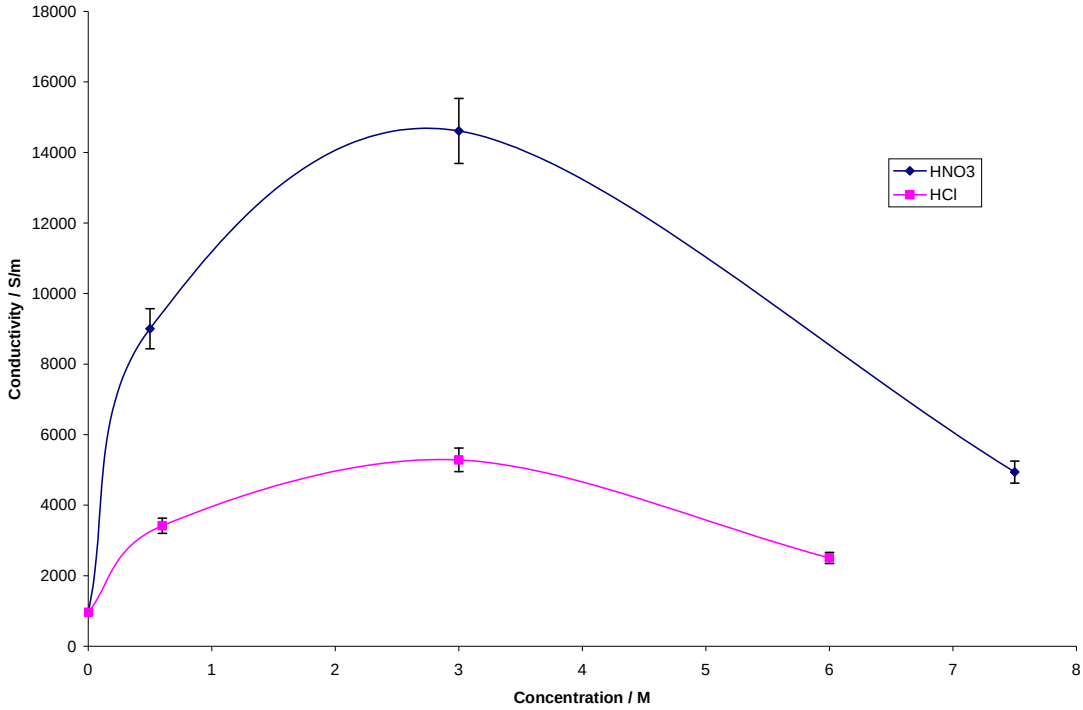

Figure 7-6 – Graph depicting conductivity of carbon fibre after acid doping

7-3-2-7 Rationalisation of Doping Results[2]

It is seen from the results discussed in Sections 7-3-2-1, 7-3-2-2 and 7-3-2-3, that, in all cases of polypyrrole doping, the conductivity has the biggest increase when the material is exposed to 6 M HCl. Only a very small increase was found in the case of the Aldrich material, which was unsurprising as this material was already doped.

The HCl causes protonation of the nitrogen to occur, leading to the production of the molecule depicted in Figure 1-17. In the case of nitric acid doping, it is understood that polypyrrole is an electron rich molecule, and as such is sensitive to oxidation. Therefore, when polypyrrole is doped in nitric acid, it was seen that the 2 M solutions were, in the case of the Aldrich and the BASF materials, sufficiently oxidising to cleave apart the double bonds, leading to a loss in the conjugation of the system, and therefore a huge reduction in the conductivity, see Figure 1-17. In the case of the synthesised polypyrrole it was seen that HNO_3 was actually found to increase the conductivity, this has been attributed to the increased mobility of the nitrate in this system.

In the case of the carbon fibre, protonation of the external nitrogens will occur in the case of both acids. The reaction for HCl is seen in Figure 7-8, the same reaction is seen to occur in the case of HNO_3. Although the same reaction is occurring, and similar concentrations of acids are involved, the results, outlined in Section 7-3-2-6, show that HNO_3 causes a much higher level of conductivity than HCl.

Carbon fibre samples, first surface treated with HCl and HNO_3, were analysed in a study carried out by Nohara *et al*.[2] It was seen from SEM observations that the HCl caused no significant differences to the topography of the surface, and no defects were introduced. The HCl is limited to quaternisation of, and oxidative attack of, the nitrogen nearest the surface of the fibres.

By comparison, the carbon fibres which were treated with HNO_3 showed increased surface roughness and etching. The results led the author to conclude that oxidation using nitric acid increased the total acidic functions present on the surface to a much higher extent that the HCl. This is no doubt leading to greater acidity of the nitric acid in this case. This work has proved to be highly interesting and the principles behind the doping may be employed for the nanocontaining systems.

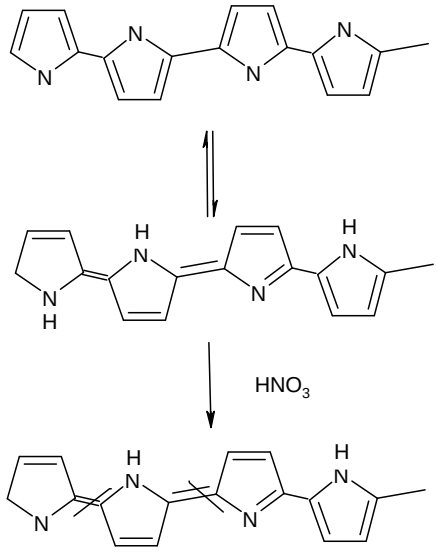

Figure 7-7 – Reaction mechanism for polypyrrole treated with nitric acid

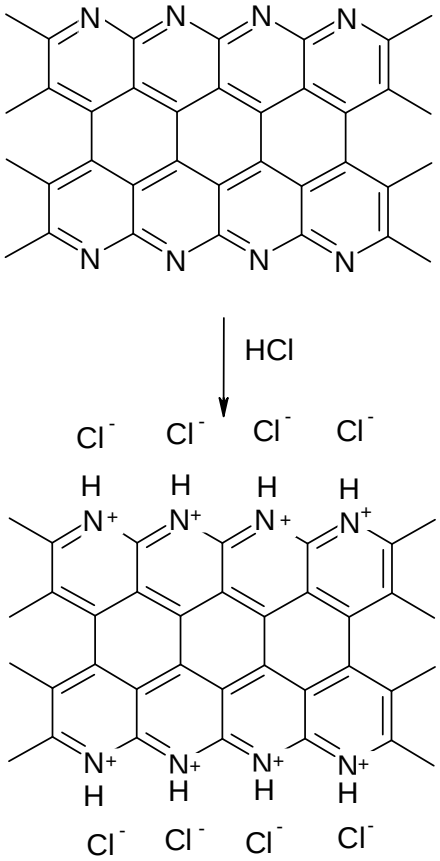

Figure 7-8 – Reaction mechanism for carbon fibre treated with nitric acid

7-3-3 Nanomaterial Results

7-3-3-1 An Initial Note on Errors

In order to quantify the degree of error typical of the four-point probe, 10 measurements of conductivity were carried out on the same sample. The sample chosen was a 10 % directly blended nanographite disc. The thickness of the disc was 7.17 x 10^{-4} m, with the applied current being 0.01 amps. The values of CF_1 (correction factor 1) and CF_2 (correction factor 2) were 3.7682 and 1, respectively, with the conductivity calculated using Equation 6-5. The actual error calculation is detailed in Appendix 2, where it is seen that a typical error associated with the four-point probe is 2.6 %. Therefore, this is the error which is applied to all subsequent results.

7-3-3-2 Solution Blending[3]

The PES-based co-polymer/graphite composites were sonicated in chloroform, according to the method detailed in Section 6-3-10-1. Pictures of the resultant composites, after being poured into a circular mould and dried overnight under vacuum, are shown in Figure 7-9. It is noted that the samples have a foamed up appearance. They have a porous, spongy look which becomes more pronounced as more graphite is introduced into the system, see Figure 7-10 and Figure 7-11.

Figure 7-9 – Picture of graphite composite after exposure to vacuum overnight

Figure 7-10– Picture of the bottom of 2 % graphite / PES-based co-polymer composite

Figure 7-11 – Picture of the bottom of the 80 % graphite / PES-based co-polymer composite

As was also detailed in Section 6-3-10-1, the samples were ground using an electric grinder and then pressed into discs using a 13 mm IR dye. The conductivity of these small discs was measured, in triplicate, using a four-point probe, and the resultant graph is shown in Figure 7-12. It can be seen that the percolation threshold is approximately 8 %, with the highest conductivity – 7.4-9.2 x 10^2 S/m – achieved for the 80 % loading level.

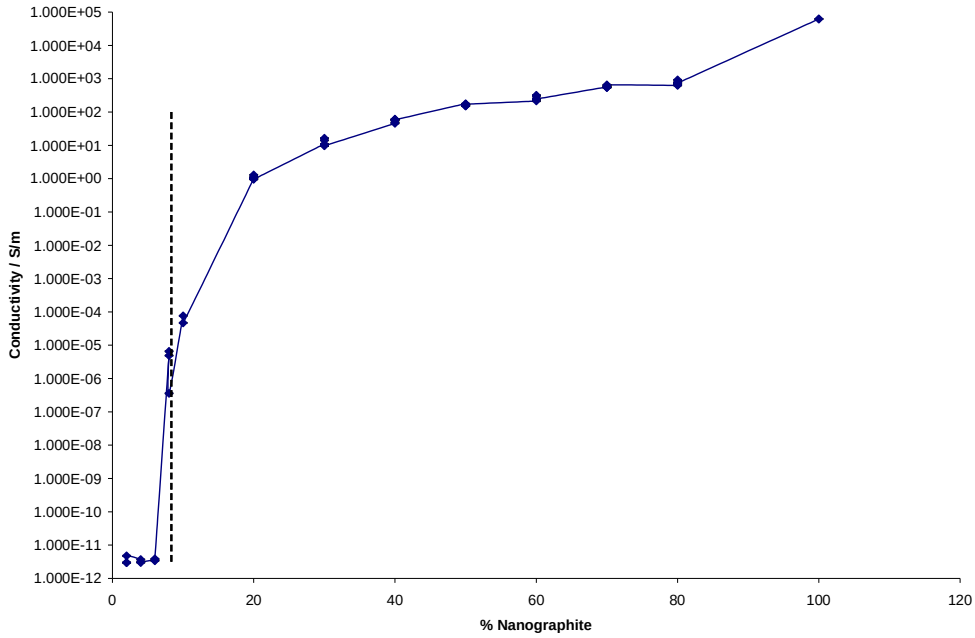

Figure 7-12 - Conductivity of solution blended nanographite discs

7-3-3-3 *In-situ* Processing

After following the procedure detailed in Section 6-3-4, the conductivity of 10 % nanographite produced *in-situ* was determined. The conductivity was seen to be 7.4 x 10^{-12} S/m. As this was much lower than anticipated, SEM analysis was carried out on a pressed disc of the material. Resultant pictures can be seen in Figure 7-13.

It can be seen from this figure that the main structures visible appears to be that of the polymer matrix, although it is seen from the microanalysis results, detailed in Table 7-18, that the % carbon present is only ~1.15 % less than would be theoretically expected. Therefore the diminished conductivity cannot be simply attributed to loss of carbon material. This extremely low conductivity suggests that even a very small quantity of polymer between the graphite platelets is enough to make the material insulating. The SEM images suggest that there is a good dispersion occurring in this case, and as such, the percolation pathway has been interrupted, leading to a very low conductivity.

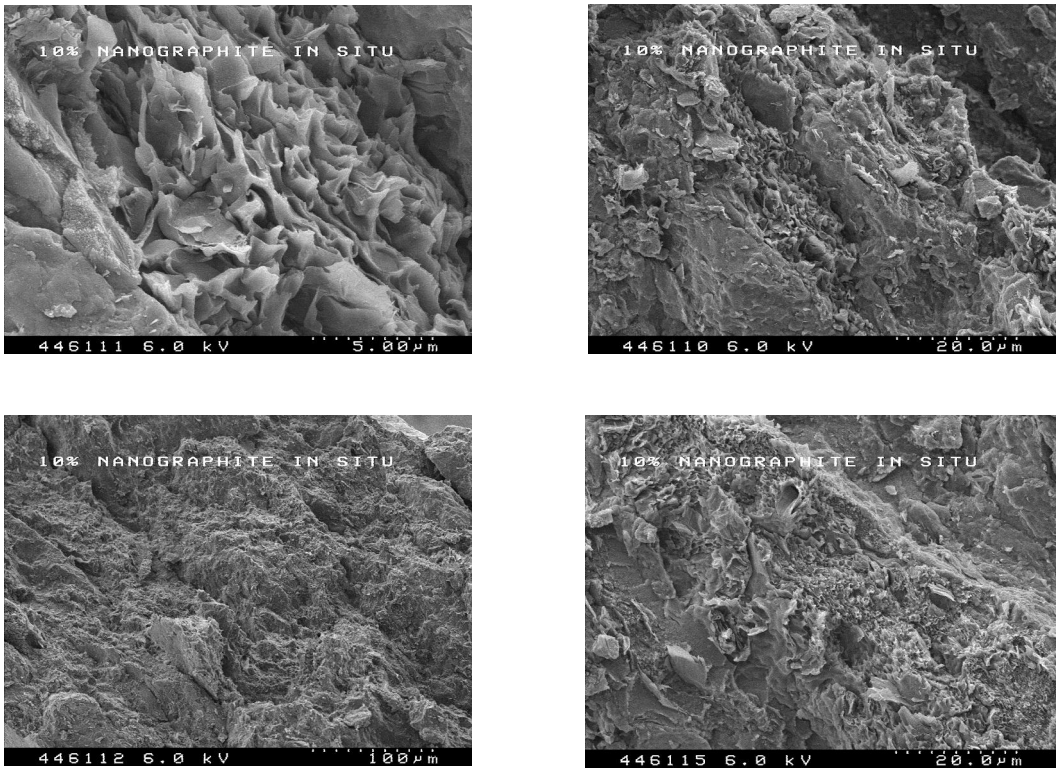

Figure 7-13 – SEM images of 10 % *in-situ* prepared nanographite sample

7-3-3-4 Direct Blending

7-3-3-4-1Nanographite Blended with PES-Based Co-Polymer [3]

For purposes of comparison direct blending of nanographite/PES-based co-polymer powders, with the same concentration as involved in solution blending, see Section 6-3-10-1, were also created. In order to ascertain the maximum possible conductivity achievable, discs of pure nanographite were also made, and can be seen in Figure 7-14. These discs were perfectly smooth and had a mirrored surface – this mirroring was difficult to capture on camera, but can be seen by looking at the third disc in Figure 7-14. Furthermore, it is noted that the pure nanographite powder compacted into much thinner discs, c.f. the same mass of powder, than any other material utilised in this project.

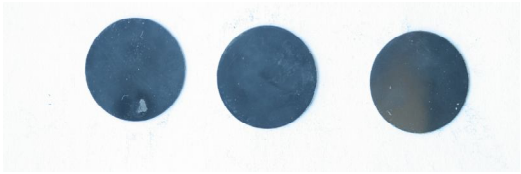

Figure 7-14 - Picture of pure graphite discs

The conductivity achieved can be seen in Figure 7-15. It is seen from this figure that the conductivity increases exponentially with respect to increasing nanographite loading. The sonicated material percolates at approximately 8 % nanographite content, indicated by the dotted line, achieving a maximum conductivity value of 1 x 10^3 S/m for the 80 % nanographite composite. It is noted that the 100 % nanographite point on the graph has been included for purposes of comparison only, as it refers to the conductivity of a sample of pure nanographite.

The graph concerning the blended material is shown in Figure 7-15. Firstly, it is noted that the blended material has a much lower percolation threshold when compared to the sonicated material – 3 % c.f. 8 % – it is also noted that the conductivity of the blended sample reaches a higher value than the sonicated samples, achieving a figure of 1 x 10^4 S/m for the 80 % nanographite blend. The pure nanographite had a conductivity of 6 x

10^4 S/m. In order to put these results into perspective the conductivity of copper is 59.6 x 10^6 S/m.[4]

To determine if the quantity of carbon present in both the sonicated and directly blended samples is the same, 10 % samples of both were submitted for microanalysis – the results can be seen in Table 7-18. It can also be seen here that there is not a significant difference in carbon level, and therefore the conductivity differences must be attributed to morphological differences between the materials.

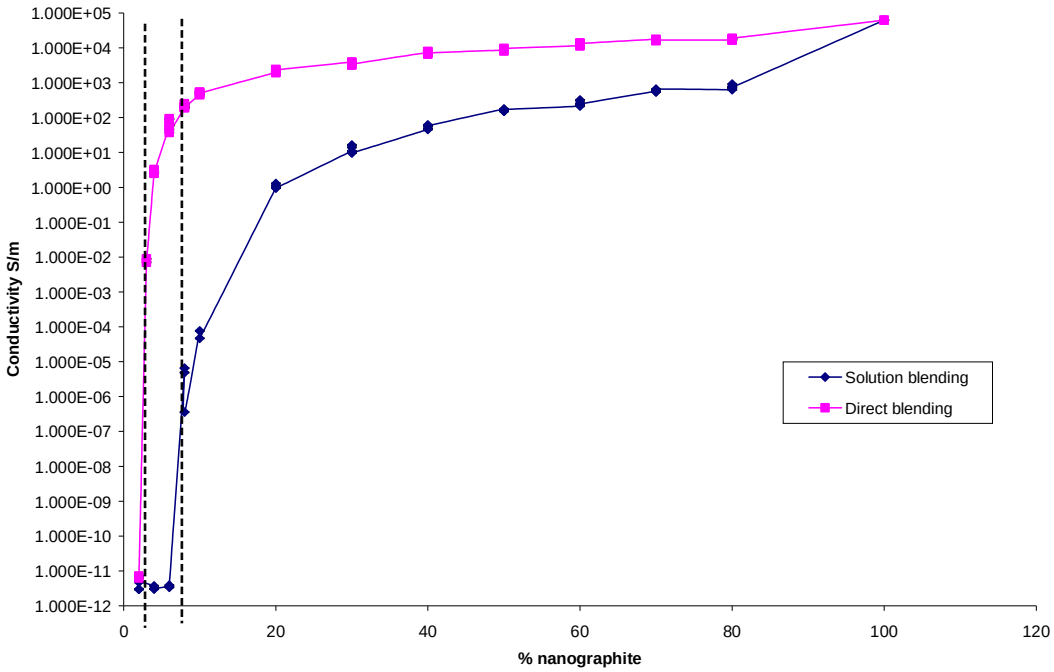

Figure 7-15 - Conductivity comparison results of solution blending composites and directly blended nanographite discs

7-2-3-4-2 Nanographite Blended with Carbon Nanotubes[3]

After carrying out the experimental procedure detailed in Section 6-3-10-2, the conductivity of increasing quantities of carbon nanotubes directly blended with a 10 % nanographite matrix was tested using a four-point probe. The resultant graph is shown in Figure 7-16. The conductivity of the pure nanotubes was found to be 8.3 x 10^2 S/m,

which is approximately 2 orders of magnitude less than the pure nanographite, which has a conductivity of 6.2 x 10^4 S/m. This conductivity difference may be due to the presence of defects within the carbon nanotubes leading to a reduction in conductivity.

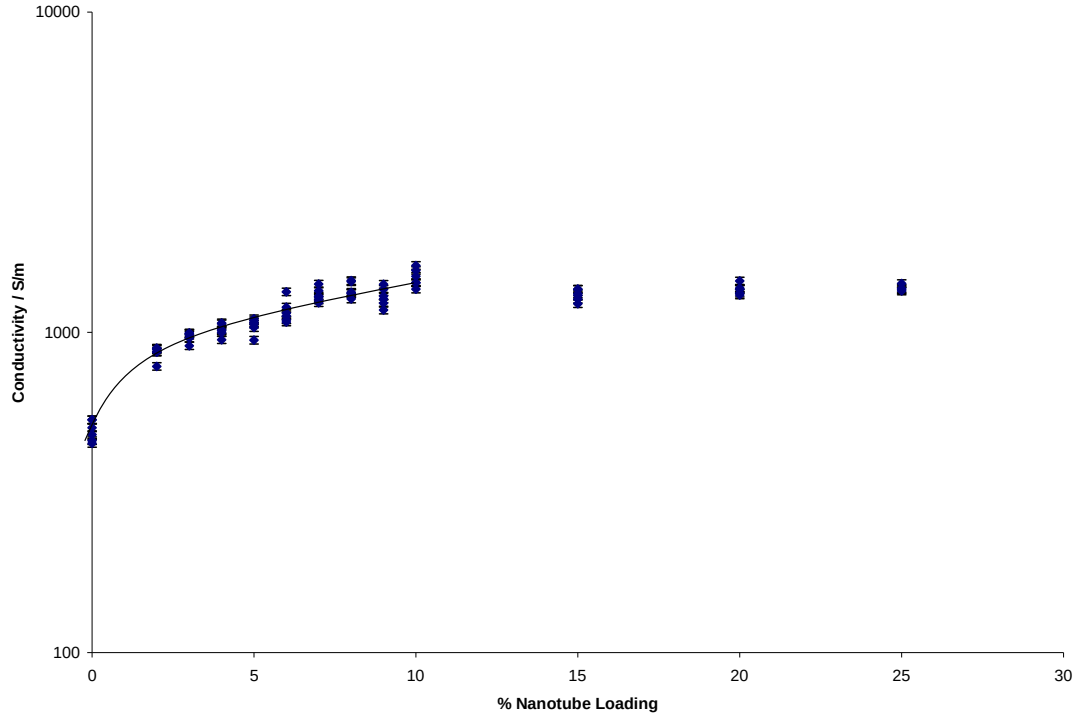

Figure 7-16 – 10 % nanographite + increasing quantities of carbon nanotubes

It is seen from Figure 7-16 that the addition of increasing quantities of nanotubes to a 10 % nanographite matrix did not effectively enhance the conductivity of the system, although there was a small steady increase in the conductivity up to a concentration of 10 % nanotubes. Starting from a base conductivity of 5 x 10^2 S/m, the conductivity rises to a value of ~ 1.45 x 10^3 S/m with the addition of 10 % nanotubes and there is no further enhancement in conductivity achieved. The small enhancement may be due to the ability of the rod-like nanotubes to bridge some gaps between the platelet structures of the nanographite.

7-3-3-4-3 Carbon Black

After following the experimental procedure outlined in Section 6-3-10-2-3, the conductivity of 10 % nanographite with increasing quantities of carbon black (Vulcan XC72 and Vulcan XC605) were obtained, and the resultant graphs are shown in Figure 7-17 and Figure 7-18. It is seen from these graphs that the conductivity actually decreases with increasing levels of carbon black in both cases. The conductivity of the pure carbon black was found to be 6.5 x 10^2 S/m in the case of the Vulcan XC72, and 4.5 x 10^2 S/m in the case of Vulcan XC605. As this is, again, less than the conductivity of the nanographite (6.2 x 10^4 S/m). It is therefore concluded that the materials are not blending together in an enhancive manner.

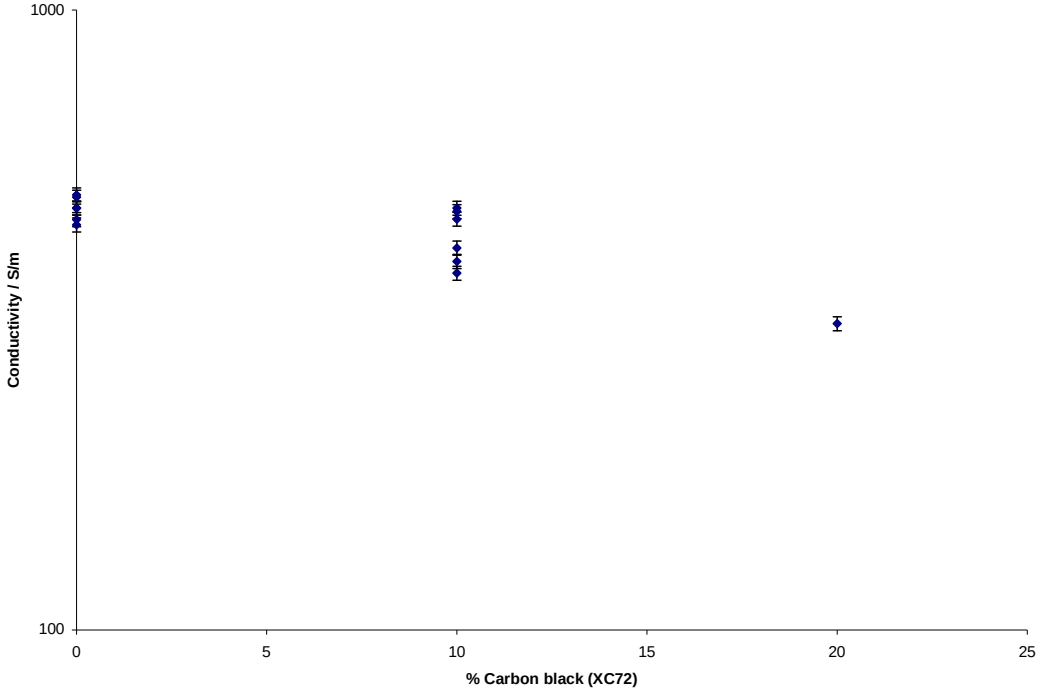

Figure 7-17 – 10 % Nanographite + increasing concentrations of Carbon Black (XC72)

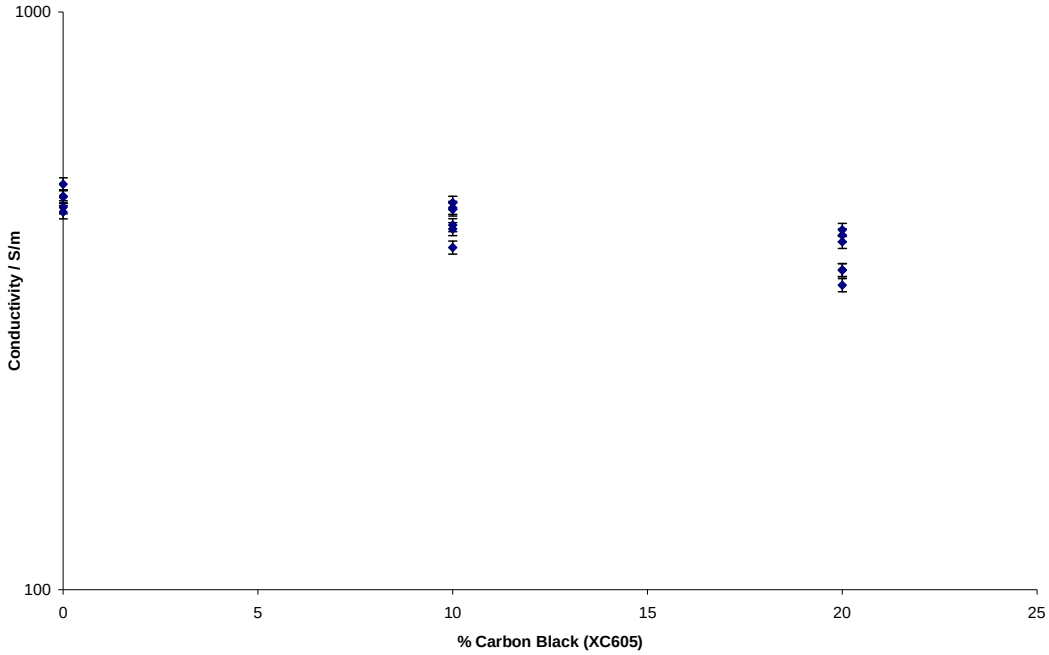

Figure 7-18 – 10 % Nanographite + increasing concentrations of Carbon Black (XC605)

7-3-3-4-4 Nanographite Blended with Phthalocyanine

After following the procedure outlined in Section 6-3-10-2-4, the conductivities of pressed discs of directly blended PES-based co-polymer/phthalocyanine were measured using a dielectric instrument. A picture of the phthalocyanine in powder form, and in pressed disc form is shown in Figure 7-19.

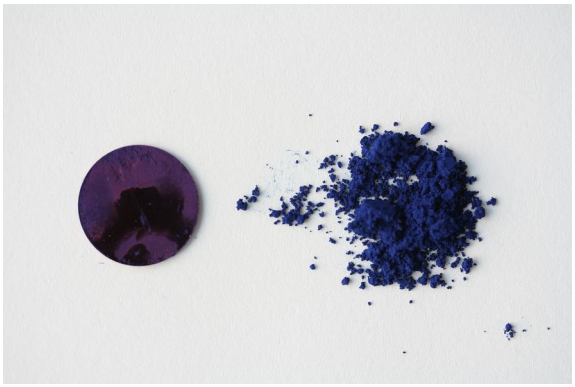

Figure 7-19 – Picture of Cu phthalocyanine in powder and disc form

It is seen from these images that the phthalocyanine powder is bright blue in colour, when the material is pressed into a disc the colour changes to more of a violet-purple. This colour change has been attributed in the past to the mono reduction of the CuPc, to form $[CuPc]^-$.[5]

After the powder was pressed into a disc, a voltage was passed through the material and the resultant current measured. The conductivity was found to be 1.7-2.2 x 10^{-11} S/m, which is obviously very low. Nonetheless, increasing quantities of phthalocyanine were blended with the 10 % nanographite material. The resultant graph is shown in Figure 7-20 where it is seen that the conductivity is not enhanced at all, and indeed the blended phthalocyanine actually has a slight detrimental effect.

It has subsequently been discovered that the counter ion for the Cu phthalocyanine complex used in this project is the phthalocyanine dianion. It may therefore be necessary to dope the phthalocyanine with a chemical such as iodine, which has been shown to improve the electrical conductivity nearly 10^{12} times that of unsubstituted copper phthalocyanine.[6] The remarkable increase in conductivity has been attributed to a decrease in the metal-metal bond distance, an increase in the approach of the ideal eclipsed system, or possibly a combination of these factors.

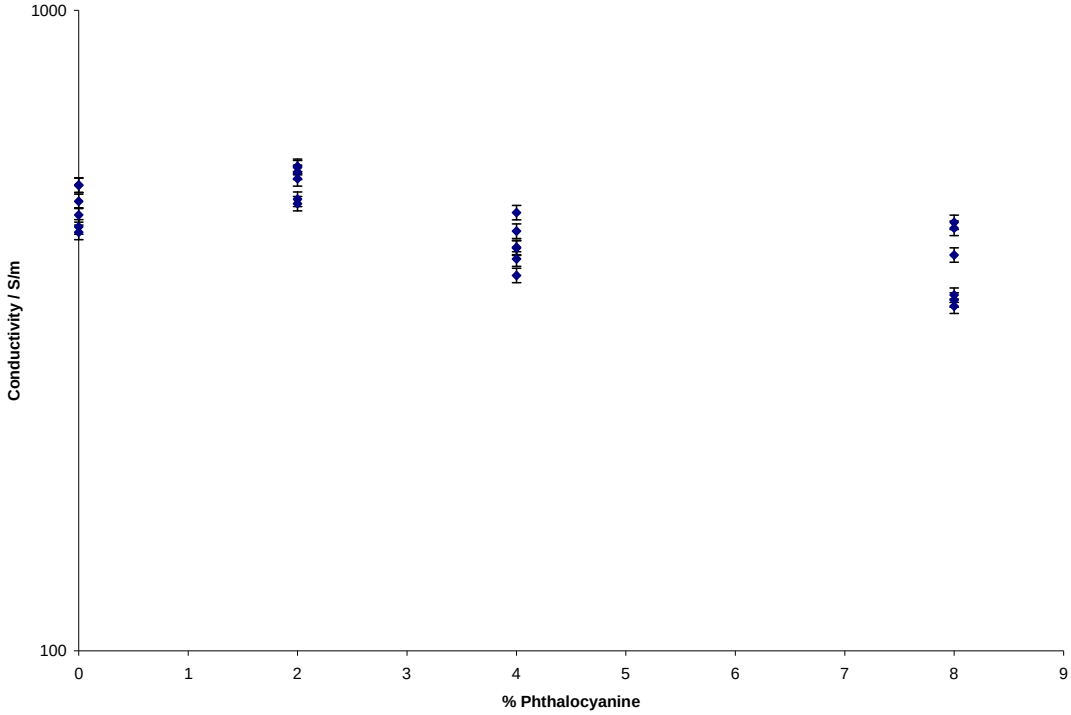

Figure 7-20 – 10 % nanographite + increasing quantities of phthalocyanine

7-3-3-4-5 TTF TCNQ

After following the procedure detailed in Section 6-3-10-2-5, the conductivity of increasing quantities of TTF TCNQ when blended with the PES-based co-polymer was investigated. The resultant conductivities can be seen in Figure 7-21 and Figure 7-22.

It can be seen from the figures that the TTF TCNQ is percolating at a level between 10-25 %. In this way it has similarities to carbon black. It can also be seen that the conductivity increases exponentially with increasing quantities of TTF TCNQ, up to a maximum value of 3.1-3.5 x 10^3 S/m. Although significantly conductive, this is still over an order of magnitude less than pure nanographite (6.2 x 10^4 S/m).

To take the investigation one step further, increasing concentrations of TTF TCNQ were blended directly with 10 % nanographite; the resultant chart can be seen in Figure 7-23. From this figure it is seen that increasing additions of TTF TCNQ leads to a steady

increase in the resultant conductivity. There is a significant jump in conductivity when 10 % TTF TCNQ was added to the 10 % nanographite polymer mixture. The conductivity rises from 4.5-5.3 x 10^2 S/m in the case of 10 % nanographite to 5.1-6.0 S/m in the case of 10 % nanographite + 70 % TTF TCNQ. It is noted that this blend is, not surprisingly, more conductive than the pure TTF TCNQ.

It has been stated in the literature that long needle-like crystals can be grown from a slow cooling technique, where the TTF TCNQ is heated until melting followed by very slow cooling in a programmable oven.[7] It was therefore decided to try to rebuild the percolation pathway in this way.

Pressed disc samples of 10 % nanographite + 20 % TTF TCNQ were chosen and were exposed to an oven at a temperature of 240°C (15°C above the melting temperature of TTF TCNQ, as seen from the material data sheet and also from the DSC curve shown in Figure 7-24) for a period of 1 hour before cooling to 200°C over a period of time, varying from 6 hours to 24 hours. The experiment was carried out in triplicate.

It was seen that the physical appearance of the discs change after exposure to heat, with the appearance of large eruptions on the surface, see Figure 7-25. As these eruptions do not appear when discs of pure nanographite are exposed to heat it can be presumed that they are wholly due to the inclusion of TTF TCNQ in the blend. These surface eruptions were seen to be more prevalent at the faster cooling rates, with much smaller eruptions occurring at the longer cooling rates of 12-24 hours.

The resultant conductivities of the discs can be seen in Figure 7-26 and Table 7-12. It is seen that the conductivity of the neat material is 2.0-2.2 x 10^3 S/m. It can clearly be seen that the cooling rate is having an enhancive effect upon the conductivity, with the conductivity rising from 8.5 x 10^{-2} – 1.5 x 10^{-1} S/m to 9.8 – 1.5 x 10^1 S/m when going from a cooling rate of six hours to a cooling rate of 24 hours. In conclusion, there does appear to be a connection between the growth of the TTF TCNQ crystalline phase and the cooling rate, with a slow cooling rate favouring the growth of larger crystals. SEM

images of TTF TCNQ, and of 10 % nanographite + 20 % TTF TCNQ before, and after, exposure to the oven at 240°C for an hour can be seen in Figure 7-27, Figure 7-28 and Figure 7-29, respectively.

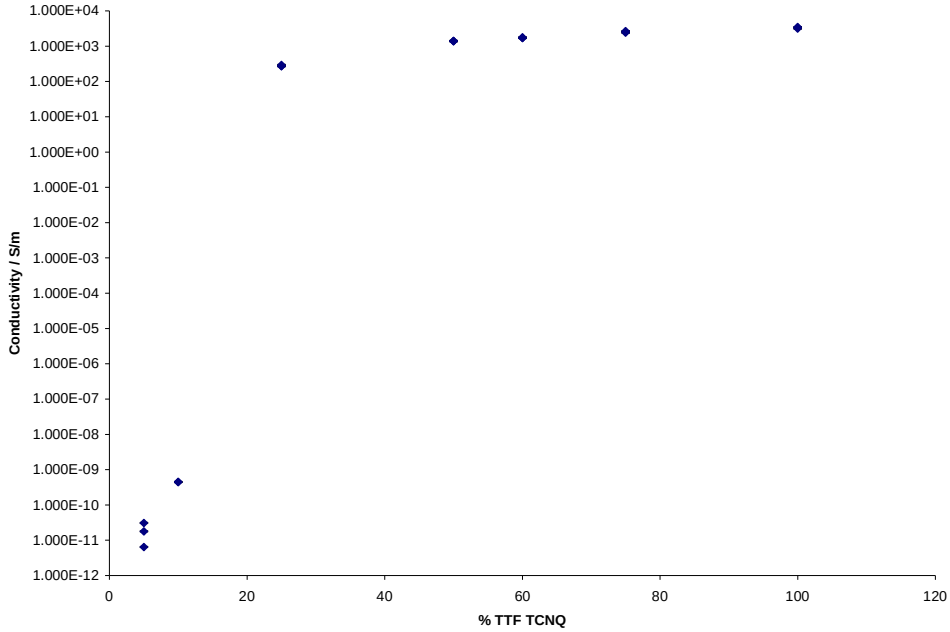

Figure 7-21 – Conductivity of increasing quantities of TTF TCNQ/PES-based co-polymer

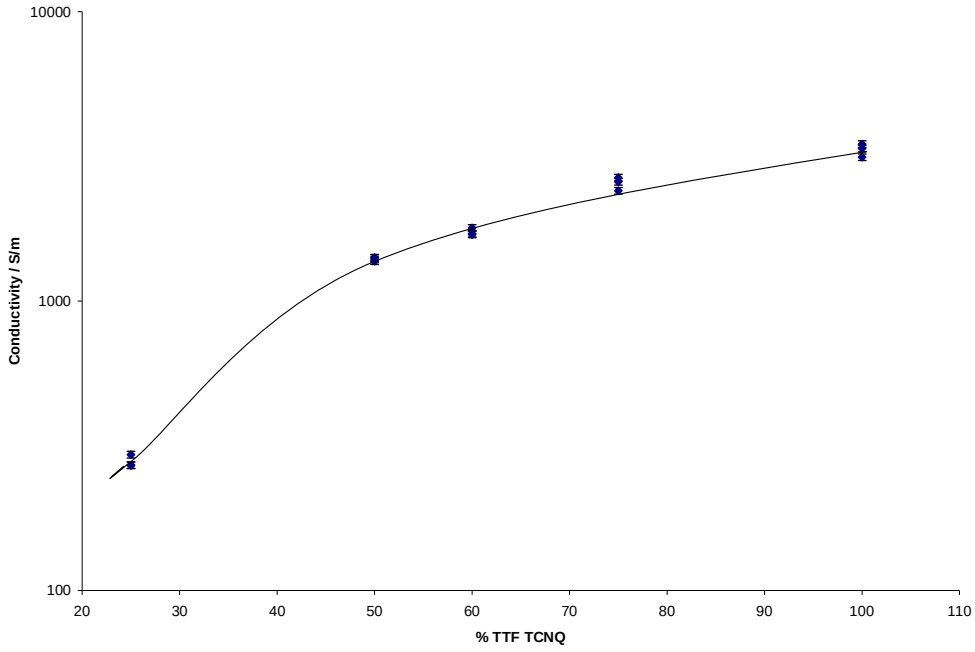

Figure 7-22– Conductivity of increasing quantities of TTF TCNQ/PES-based co-polymer focusing on higher conductivity levels

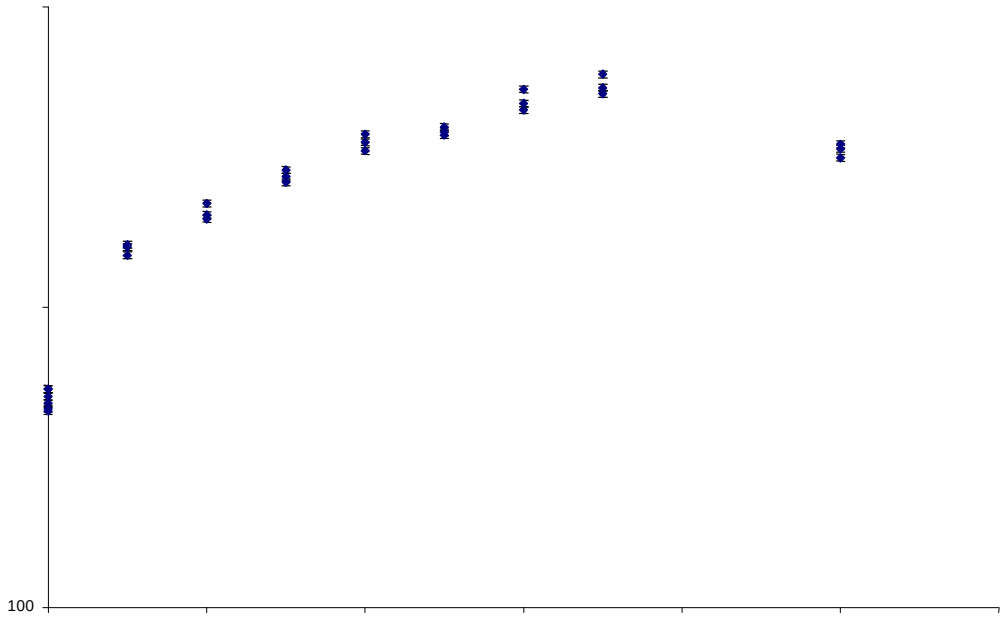

Figure 7-23– Conductivity of 10 % nanographite/PES-based co-polymer + increasing concentrations of TTF TCNQ

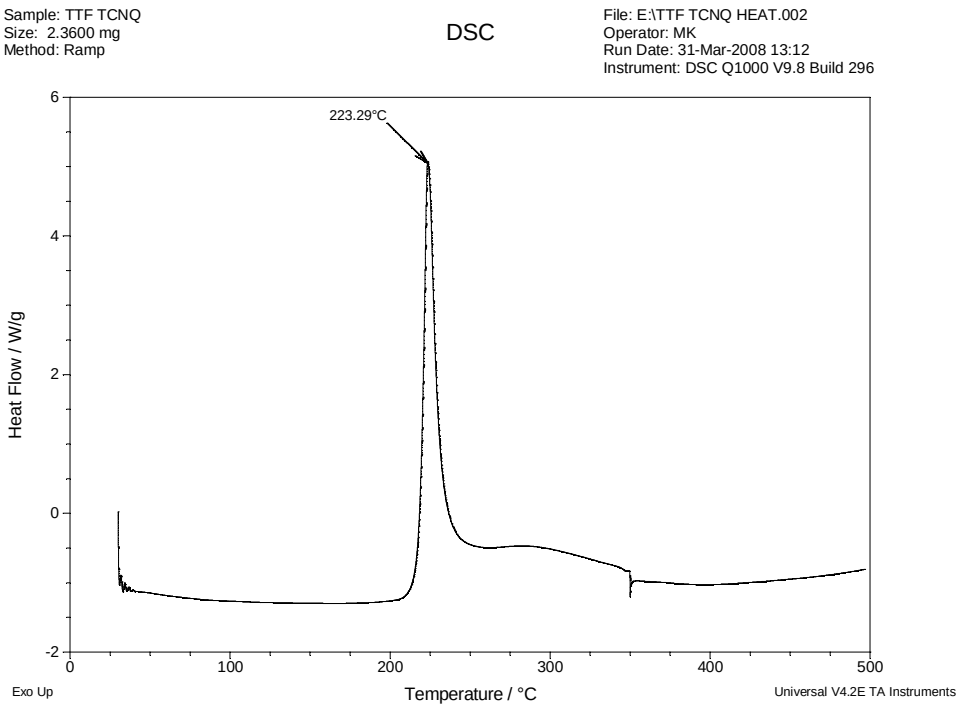

Figure 7-24– DSC trace of TTF TCNQ

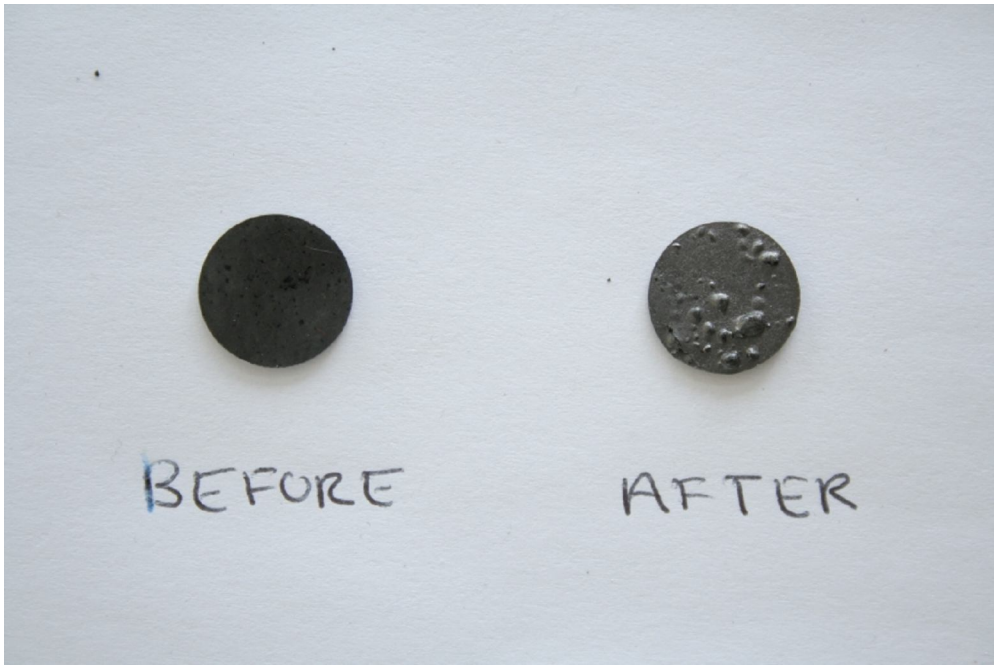

Figure 7-25 – 10 % nanographite + 20 % TTF TCNQ before and after exposure to oven at 240°C

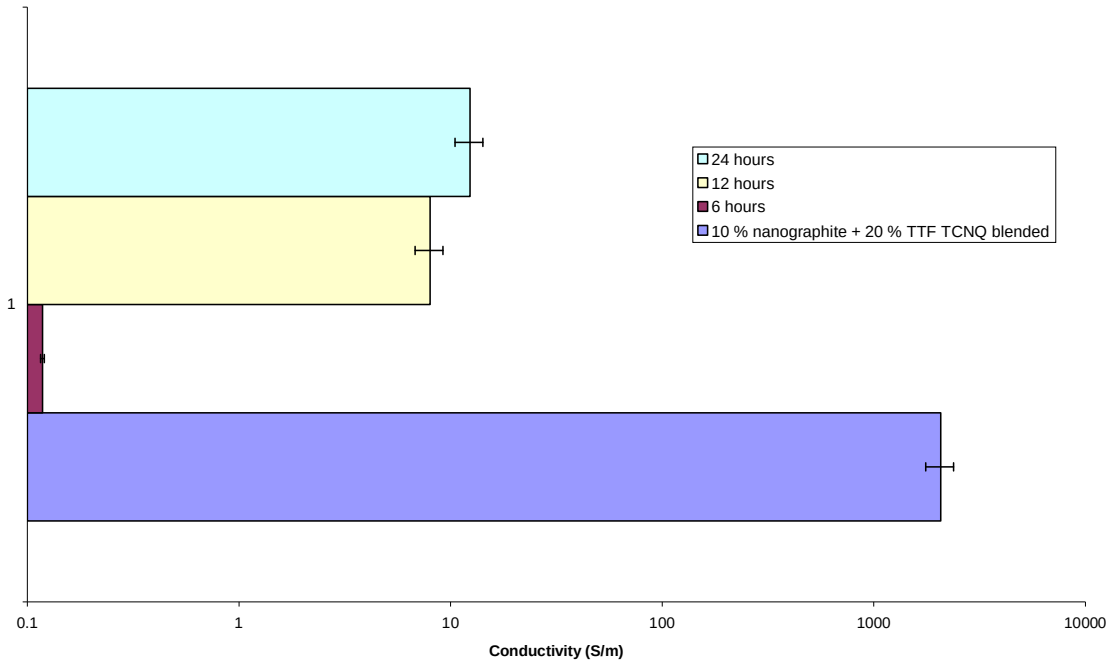

Figure 7-26- 10 % nanographite + 20 % TTF TCNQ disc conductivities after exposure to oven at 240°C for 1 hour with increasing cooling rates

Table 7-12– Conductivities of nanographite + 20 % TTF TCNQ discs after exposure to oven at 240°C for 1 hour with increasing cooling rates

Cooling rate	Conductivity (S/m)
Neat material	$2.0\text{-}2.2 \times 10^{3}$
6 hours	$8.5 \times 10^{-2} – 1.5 \times 10^{-1}$
12 hours	$5.4 – 9.9 \times 10^{0}$
24 hours	$9.8 \times 10^{0} – 1.5 \times 10^{1}$

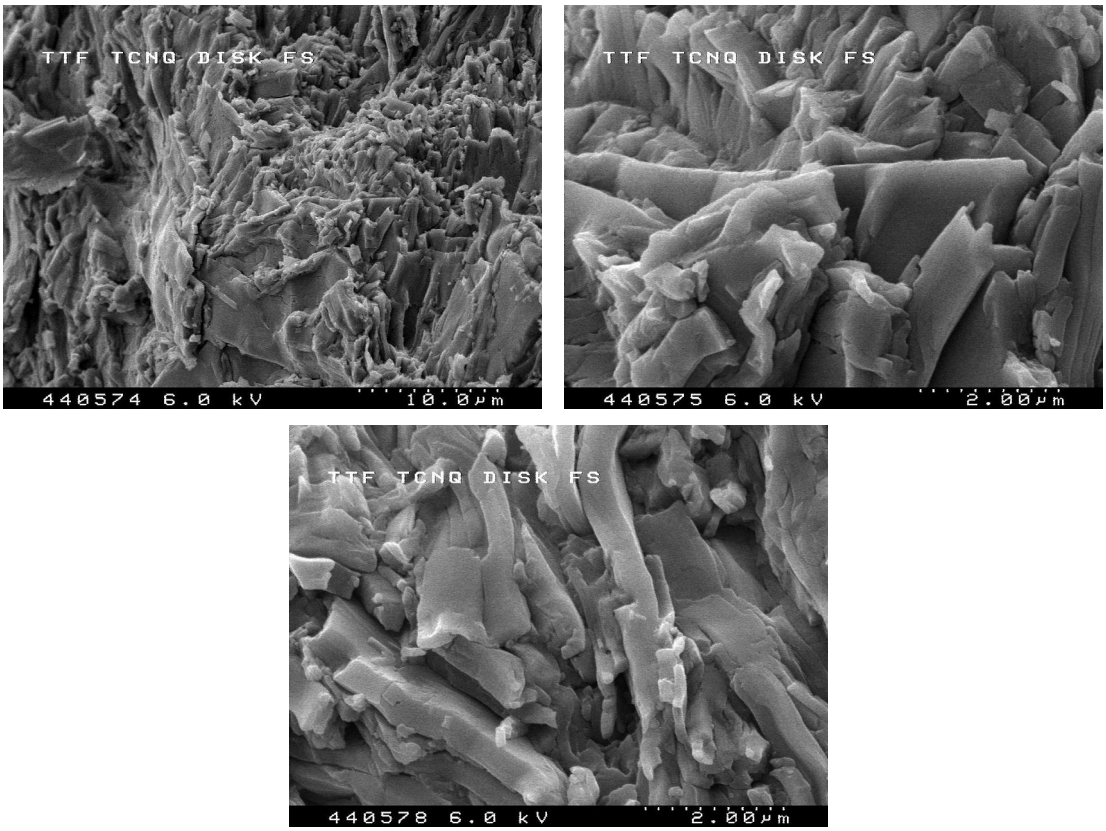

Figure 7-27 – SEM images of TTF TCNQ discs

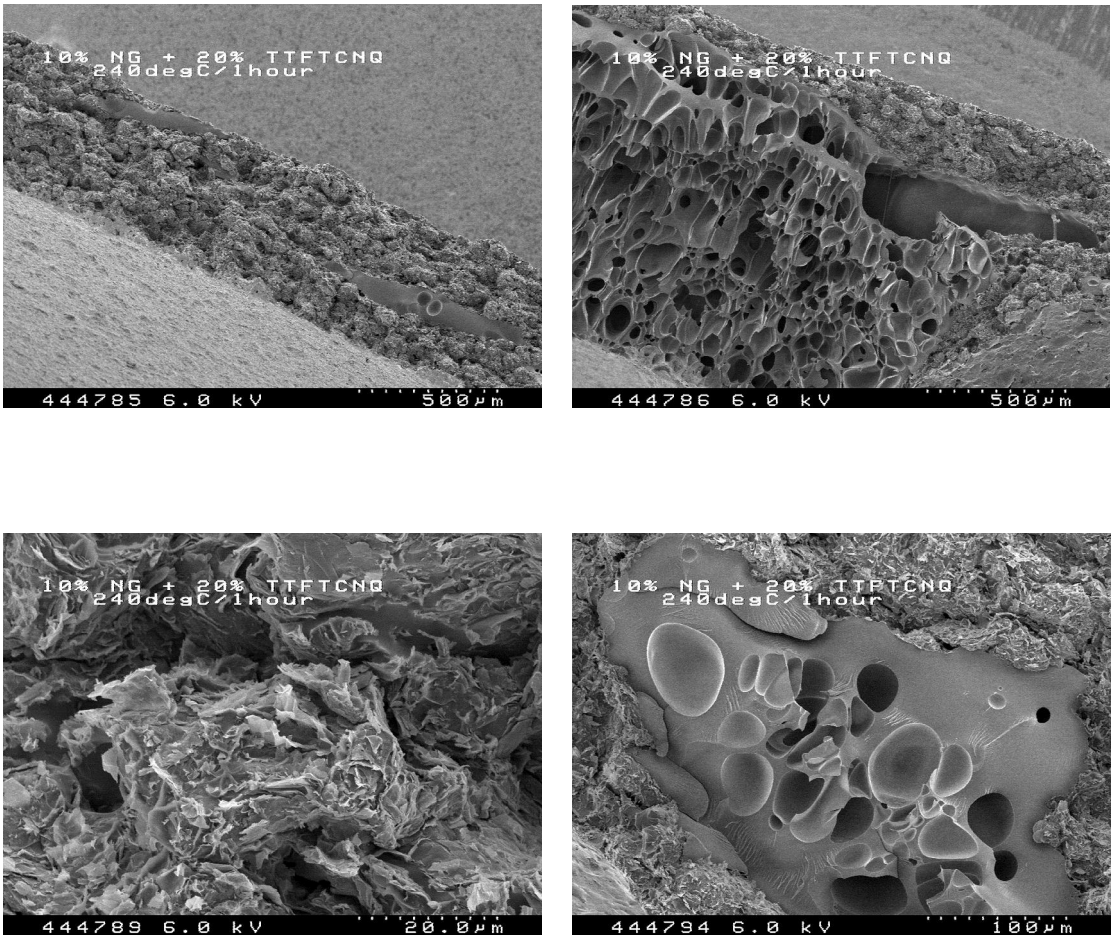

Figure 7-28 – SEM images of 10 % nanographite + 20 % TTF TCNQ after exposure to oven for one hour

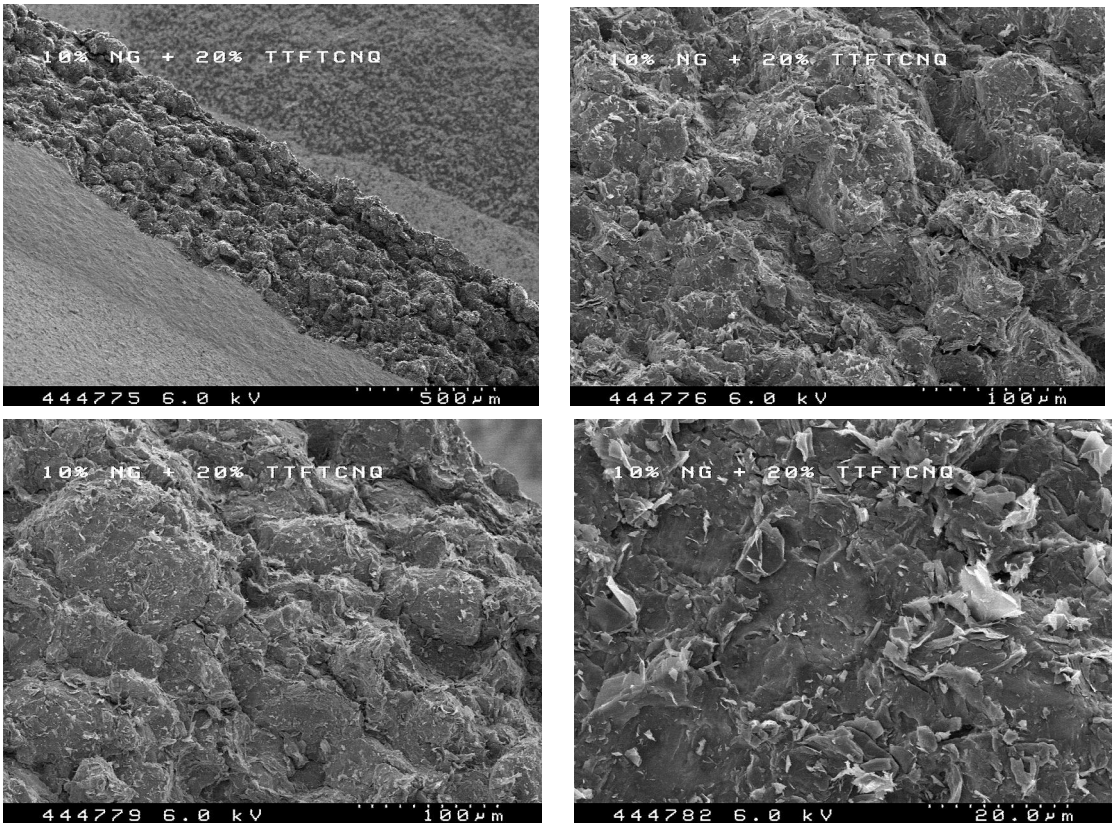

Figure 7-29 – SEM images of 10 % nanographite + 20 % TTF TCNQ discs

7-3-3-5 Epoxy

After following the procedure detailed in Section 6-3-8 – with the addition of 10 wt% nanographite – the conductivity of the resultant epoxy disc was measured. It was found to be 6.8-7.5 x 10^{-3} S/m. This conductivity is twice as high as that obtained when 10 % nanographite was introduced into a styrene/polyester matrix. In this case a conductivity of 2.5-2.9 x 10^{-3} S/m is reported. This is obviously much less than the conductivity of the directly blended nanographite / PES-based co-polymer material which was found to have a conductivity of 4.5-5.3 S/m. Since the intrinsic conductivity of the nanographite is the same the differences must reflect the influence of the matrix on the charge transport behaviour.

7-3-3-6 TGA

Thermogravimetric traces for PES-based co-polymer and commercial Radel A-100 are reproduced in Figure 7-30 and Figure 7-31. Rapid mass loss occurred in the neighborhood of 550-630°C in both polymers when exposed to an argon atmosphere. Rapid mass loss occurred in the region of 520-610°C in both polymers when exposed to air, and also at 650-710°C, which is indicative of a shift in the dominant degradation mechanism at this temperature, see derivative graph in Figure 7-32. In an argon atmosphere approximately 40 %, by mass, of the initial sample was retained up to 800°C.

In the case of the sonicated nanographite composites, shown in Figure 7-33 there is an initial degraditive drop stretching from 170 to 210°C. This fall is responsible for a reduction in mass of ~10 %. It is noted that this mass loss stretches over the T_g of the polymer. As the temperature is quite low for chain scission, and also due to the fact that composite stability is maintained for a few hundred degrees after this initial drop, it is concluded that the fall is not due to the polymer. It is more likely due to some residual chloroform present remaining trapped within the composite. As the composite goes through the T_g transition, the solvent can easily be liberated.

Furthermore, it is interesting to note that the level of residual chloroform present appears to be linked to the morphology of the composite. The more open structure of the composites with high concentrations of nanographite lend themselves to the easier escape of the solvent. The composites with lower concentrations of nanographite have a much tighter structure which keeps the solvent more securely trapped.

It is noted that as the concentration of nanographite increases in the sonicated samples, the thermogravimetric traces become, as expected, much more similar to the pure nanographite trace shown in Figure 7-34. In the case of the pure nanographite sample studied under air, the degradation starts to happen at approximately 550°C, with rapid

mass loss occurring at 650°C through to 800°C. In the case of nanographite under argon the degradation does not start to occur at all under the temperatures studied.

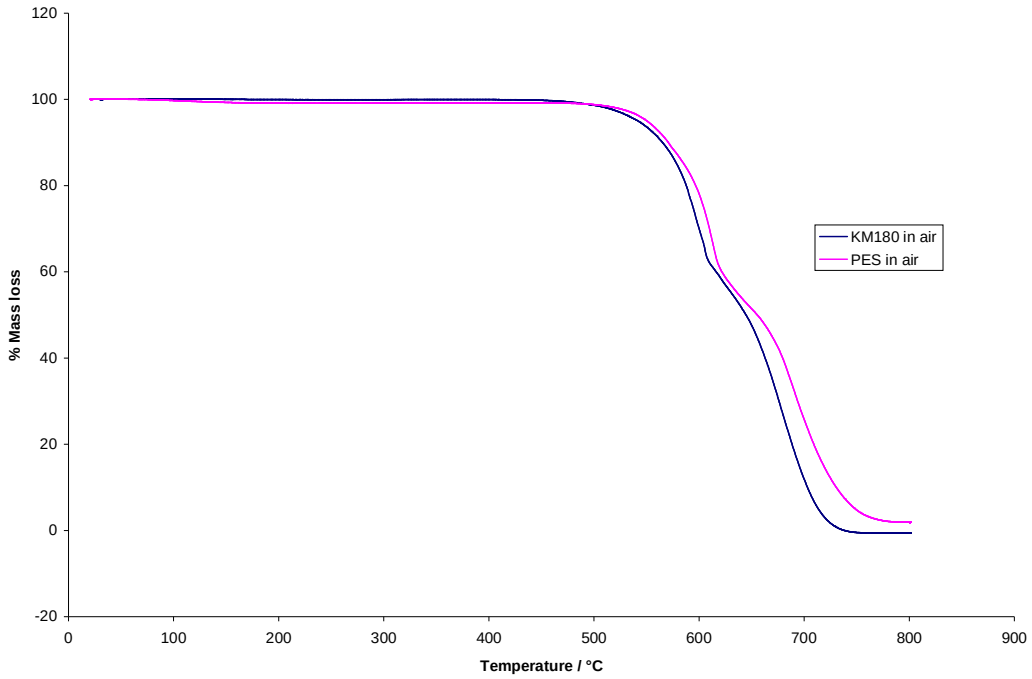

Figure 7-30– TGA of PES materials in air

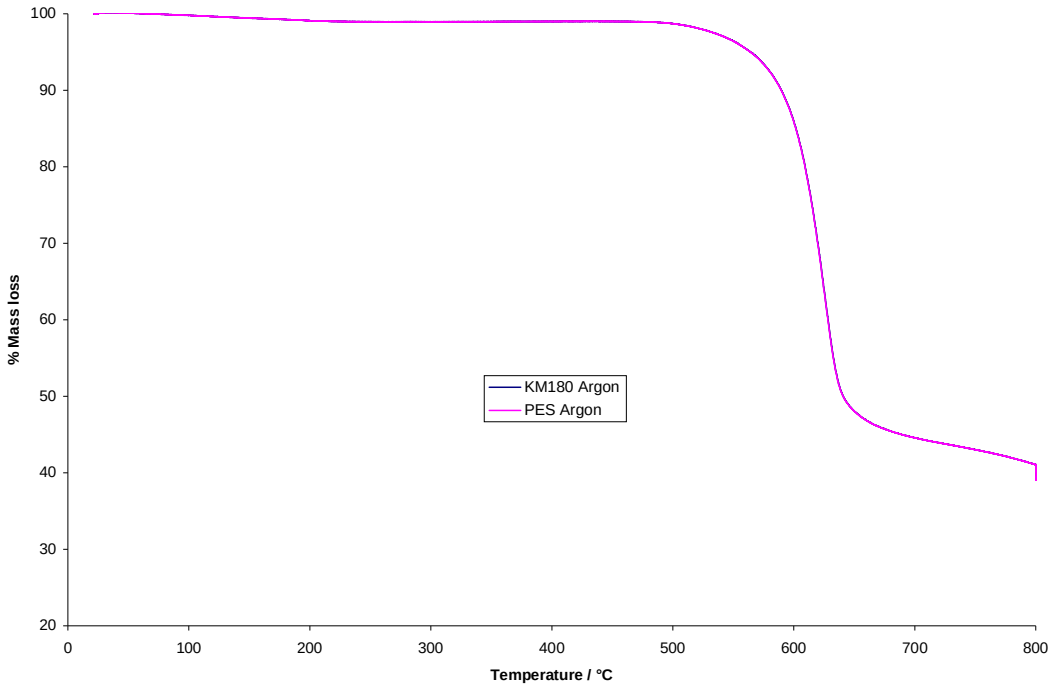

Figure 7-31 – TGA of PES materials in Argon

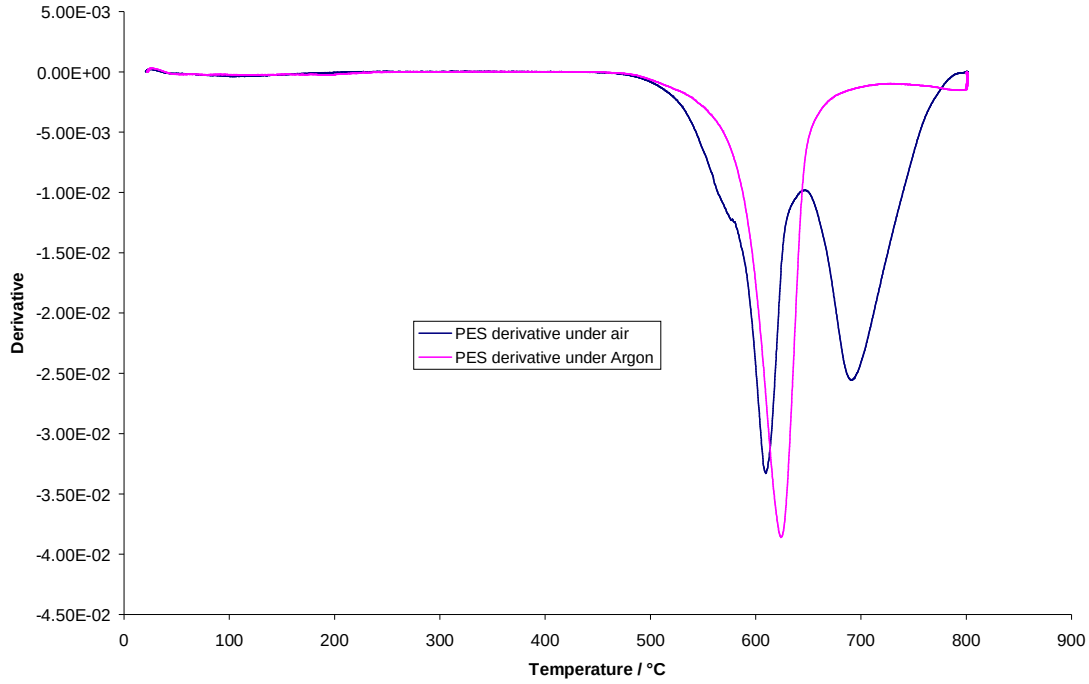

Figure 7-32– PES derivative graphs

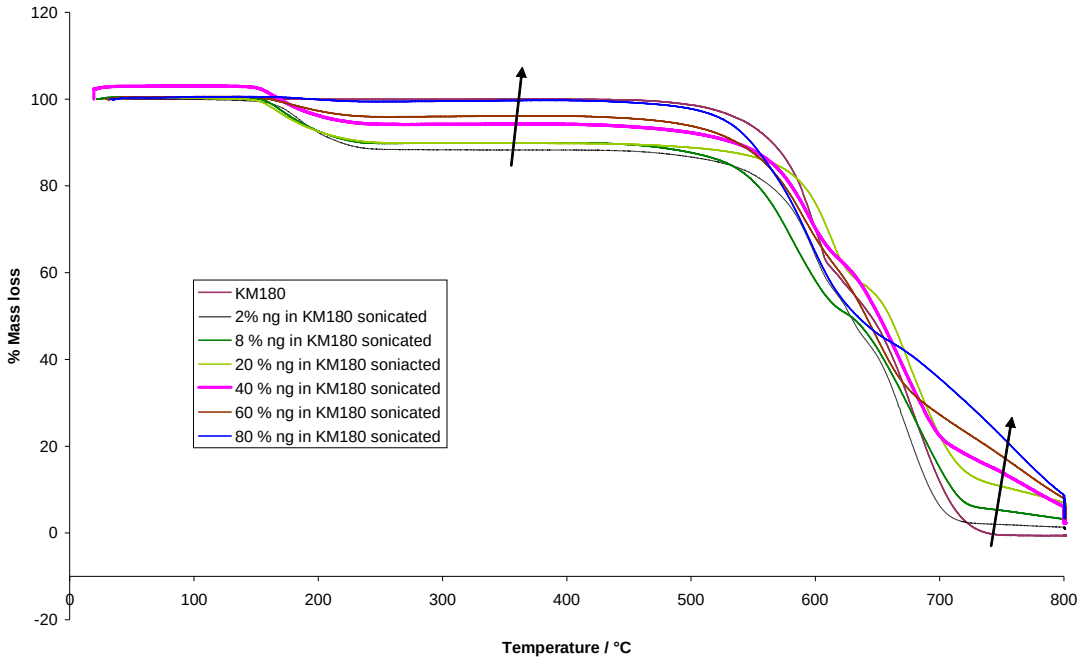

Figure 7-33– TGA of sonicated composite materials

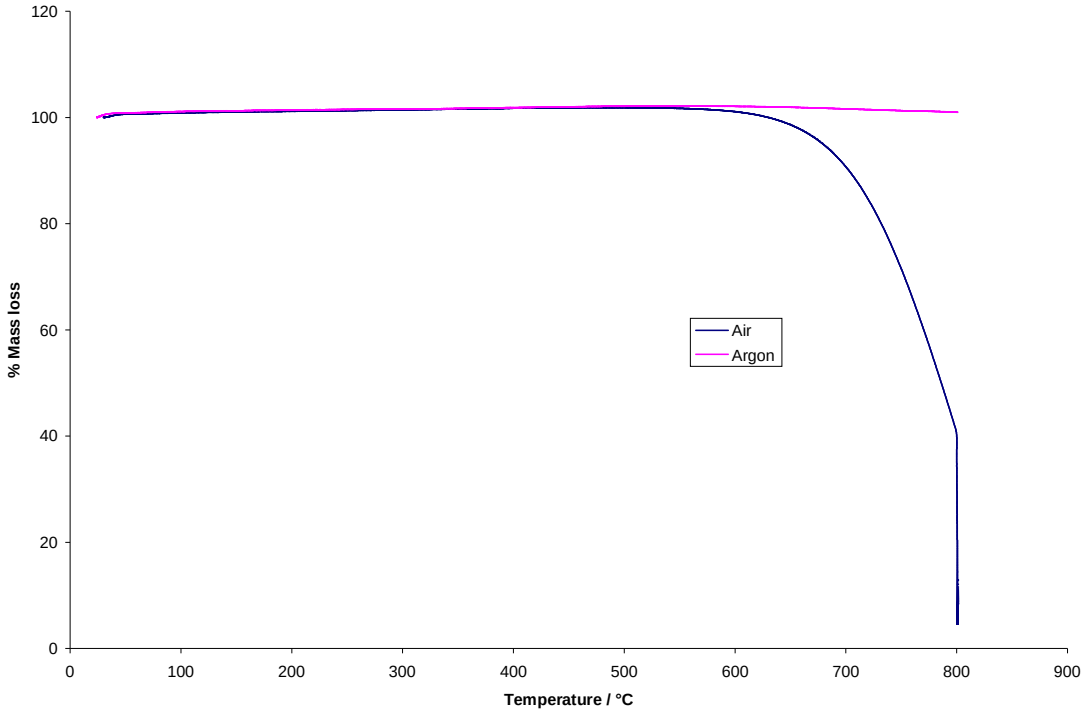

Figure 7-34 – TGA traces of nanographite under air and argon

7-3-3-7 DSC

A DSC trace showing the heat cycle of PES-based co-polymer can be seen in Chapter 5, Figure 5-2. From this graph the T_g can be seen to be occurring at ~198°C. DSC heat-cool-reheat curves for the solution blended composites can be seen in Figure 7-35, Figure 7-36 and Figure 7-37.

It can be seen from both Figure 7-35 and Figure 7-37 that there is a distinct difference in both the heating graphs. There is a poorly defined, noisy peak at approximately 150°C in Figure 7-35 which is not present in the reheat curves shown in Figure 7-37, where only a T_g can be seen at 198°C. It is deduced that the noisy peak is most likely due to residual chloroform present within the composite escaping as the material softens at the T_g.

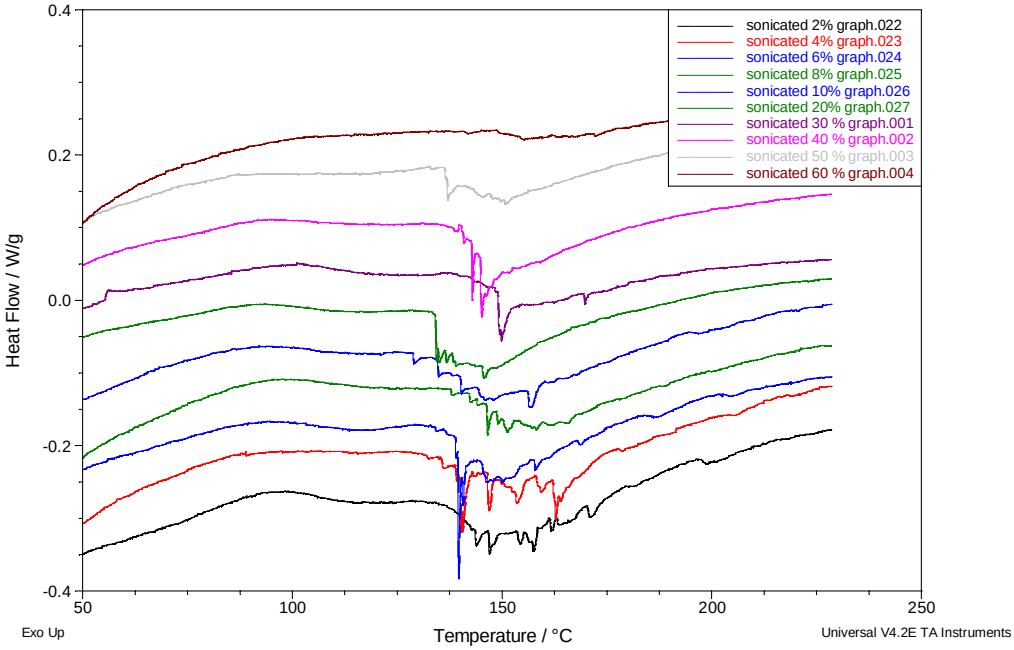

Figure 7-35 – Composites heat graphs

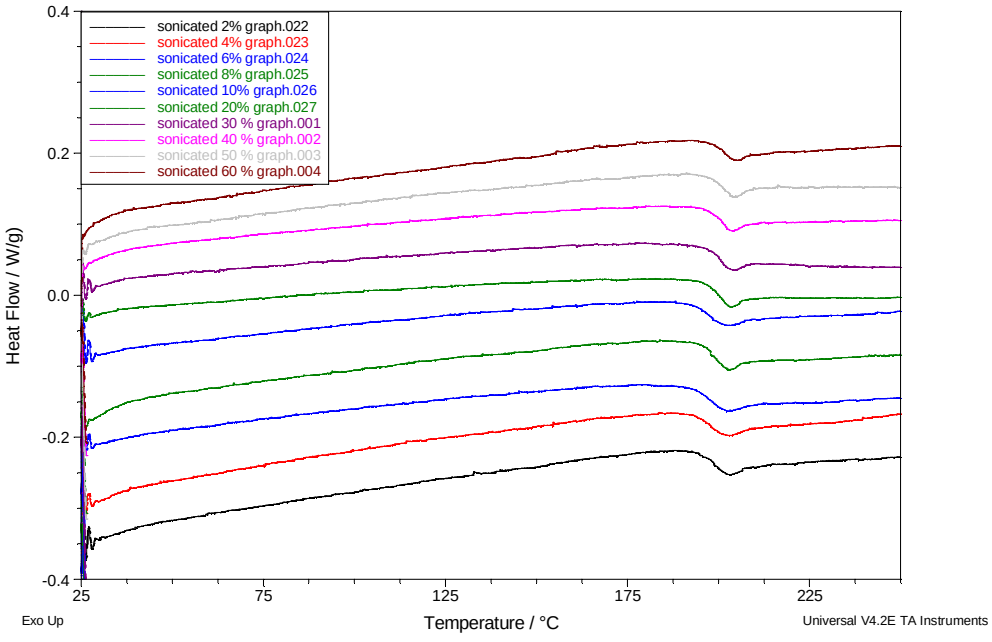

Figure 7-36 – Composites cool graphs

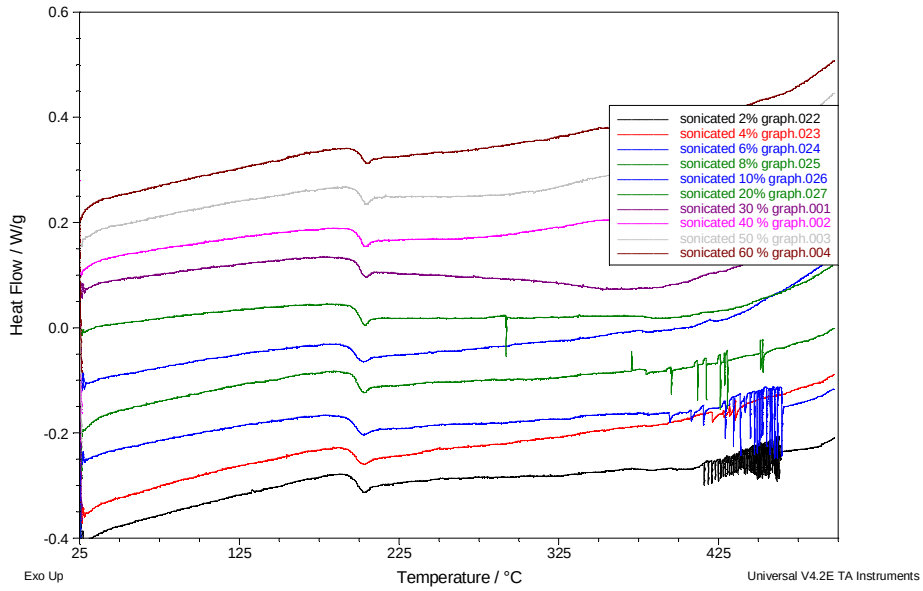

Figure 7-37 – Composites reheat graphs

7-3-3-8 SEM[3]

The images of the nanographite powder shown in Figure 7-38 (A) and (B) and Figure 7-39 (A) and (B) serve to illustrate that the nanographite particles are irregular in shape and varied in size, in general having a length of around a few to a few tens of micrometres. A typical width is more difficult to ascertain as illustrated in Figure 7-39, the particles appear to be densely packed, and the close proximity of the particles to one another makes it difficult to differentiate between individual particles.

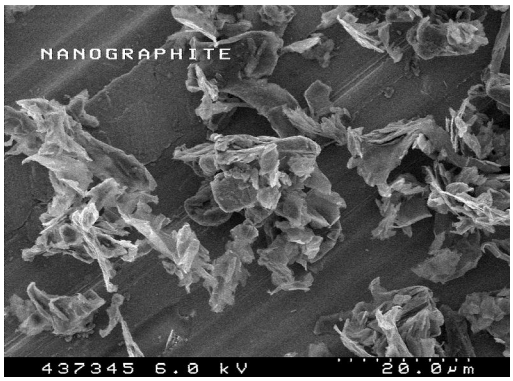

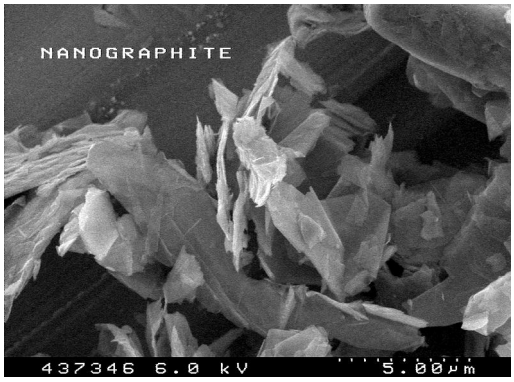

(A) **(B)**

Figure 7-38 – SEM images of nanographite powder

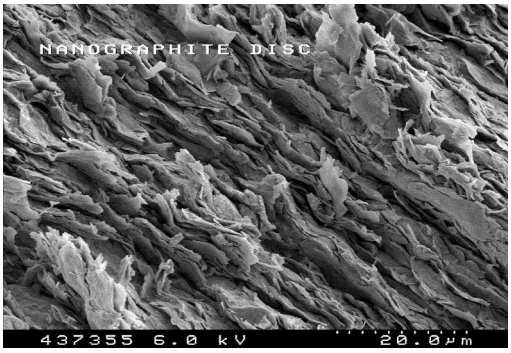

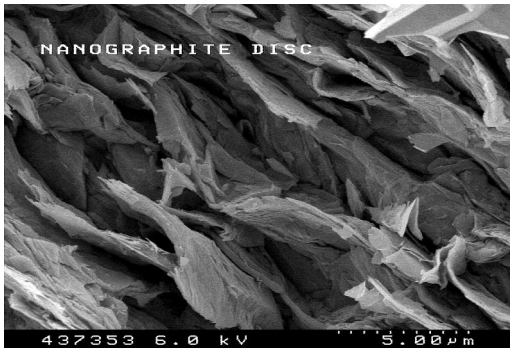

(A) **(B)**

Figure 7-39 – SEM images of nanographite discs

Examination of the 10 % nanographite/PES-based co-polymer directly blended disc, shown in Figure 7-40, Figure 7-41 and Figure 7-42, appears to show the presence of 2 separate domains, where the fracture path has gone through. Upon closer inspection, it is deduced that there is evidence of graphitic particles within the matrix domains. This is shown in Figure 7-40 (B).

These particles are dispersed within the material seen in Figure 7-40 (A), which is virtually identical to Figure 7-42 (B), identifying this phase of the system as PES-based co-polymer. Illustrated in Figure 7-41 is the fracture path travelling around, or just through, the surface of a polymer “lump”. This shows the graphite particles to be at the surface as well as distributed throughout.

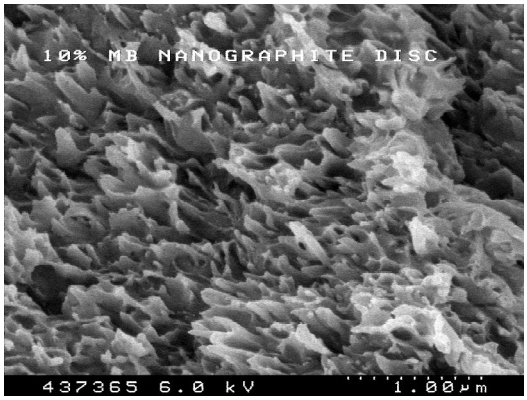

(A) **(B)**

Figure 7-40 – SEM images of 10 % nanographite blended with PES-based co-polymer

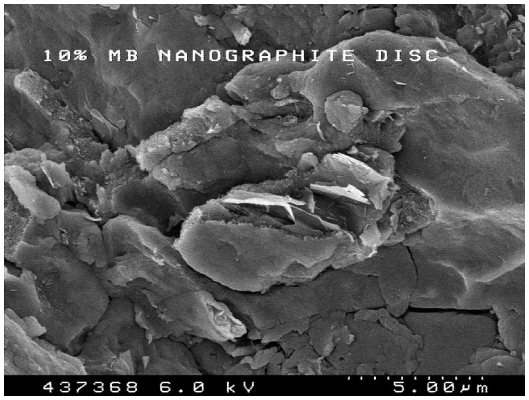

(A) **(B)**

Figure 7-41 – fracture path through polymer 'lump'

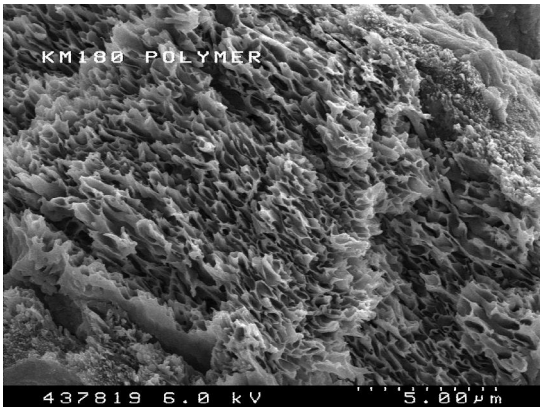

(A) **(B)**

Figure 7-42 – SEM images of PES-based co-polymer

In Figure 7-43 and Figure 7-44, SEM images of 4 % sonicated and 4 % blended materials can be seen. Interestingly, at 4 % the sonicated material is below the percolation threshold, whereas at 4 % the blended material is above the percolation threshold.

There is a noticeable difference in the SEM images of both. Firstly, it is observed that the SEM images of the sonicated nanographite material do not contain much detail i.e. a small amount of graphite flakes can be observed, but the background is sparse. Comparing this with the blended material it is seen that the images are very much more detailed, with both nanographite and polymer clearly visible.

Secondly, the nanographite in the sonicated composite appears to be shorter, therefore lowering the aspect ratio, and any property enhancement associated. Typically the length is approximately 4 μm, compared with approximately 8 μm for the blended nanographite. The disparity between the two materials is most likely directly attributable to the presence of residual chloroform in the sonicated composite.

SEM images of 10 % nanographite + 10 % nanotubes in PES-based co-polymer are shown in Figure 7-45, Figure 7-46 and Figure 7-47. It is seen that both the nanomaterials can be easily identified in the images. From Figure 7-47 a typical diameter of a nanotube is estimated at approximately 50 nm. From the SEM images it is noticed that the two nanomaterials exist mainly in separate regions of the blend, with the nanotubes maintaining an aggregated, bundle-like structure, see Figure 7-46(A). It can also be seen that there are some instances where the small tube-like structures of the nanotubes do act as mini wires connecting the nanographite platelets, as can be seen in Figure 7-47. The small increase in conductivity seen in the blend is attributed to this morphological enhancement effect. It was unfortunate that the bulk of the material did not mix together in this enhancive manner.

SEM images of 10 % nanographite blended with carbon black are shown in Figure 7-48 and Figure 7-49. Two separate carbon blacks (XC72 and XC605) were blended with the

nanographite with a view towards enhancing the conductivity. It was seen that the nanographite and the carbon black tended to exist discretely within the matrix. Both carbon blacks show a spheroidal structure, and it is quite clear that they are joined together in aggregates or clusters fusing into a continuous solid structure of carbon.

The discrete nature of the mixture is responsible for the reduction in conductivity seen in the material blends. As the carbon black has a lower conductivity than the nanographite, being 6.5 x 10^2 S/m for XC72 and 4.5 x 10^2 S/m for XC605, with the nanographite having a conductivity of 6.2 x 10^4 S/m, it is therefore unsurprising that if the materials exist discretely within a matrix the conductivity of a 10 % blend of nanographite is lowered by the addition of carbon black.

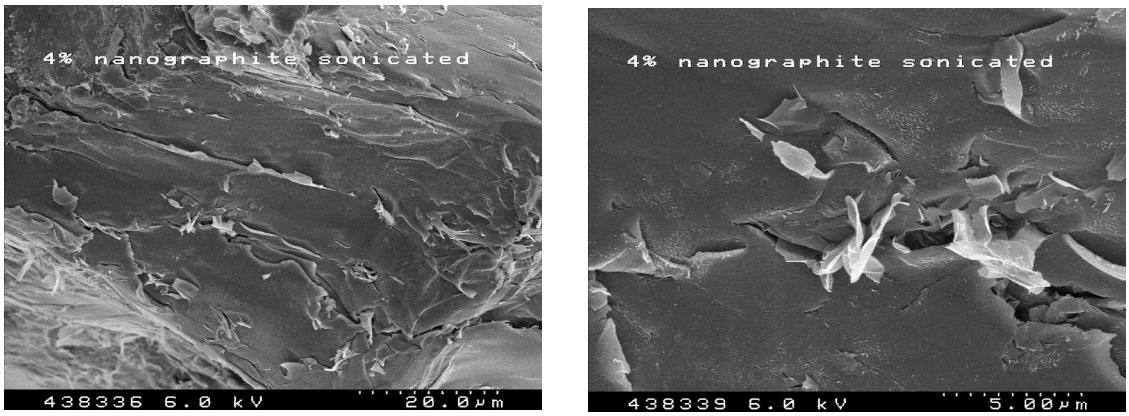

Figure 7-43– 4 % sonicated nanographite SEM images

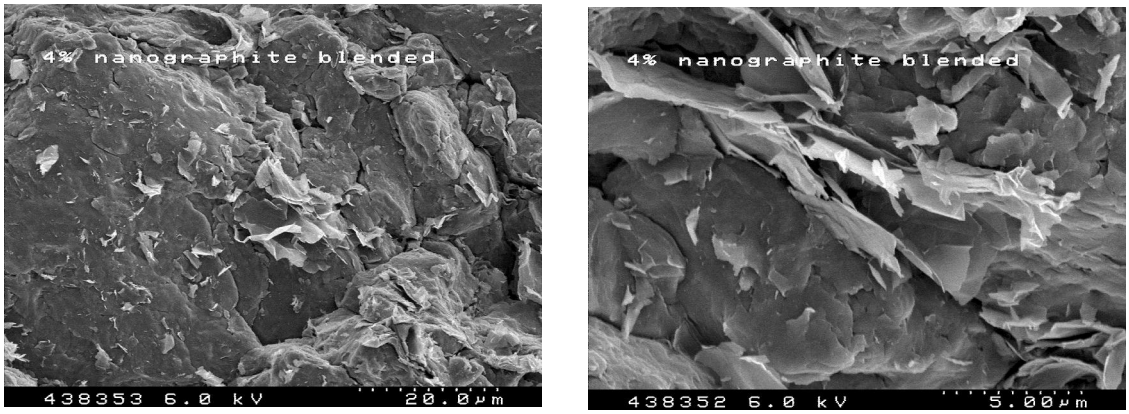

Figure 7-44 – SEM images of 4 % nanographite blended

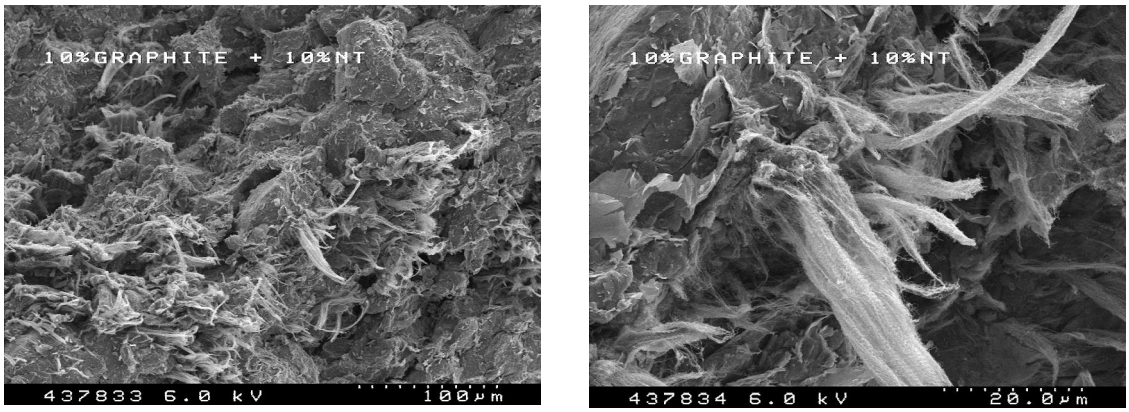

Figure 7-45 – SEM images of 10 % nanographite blended with 10 % nanotubes

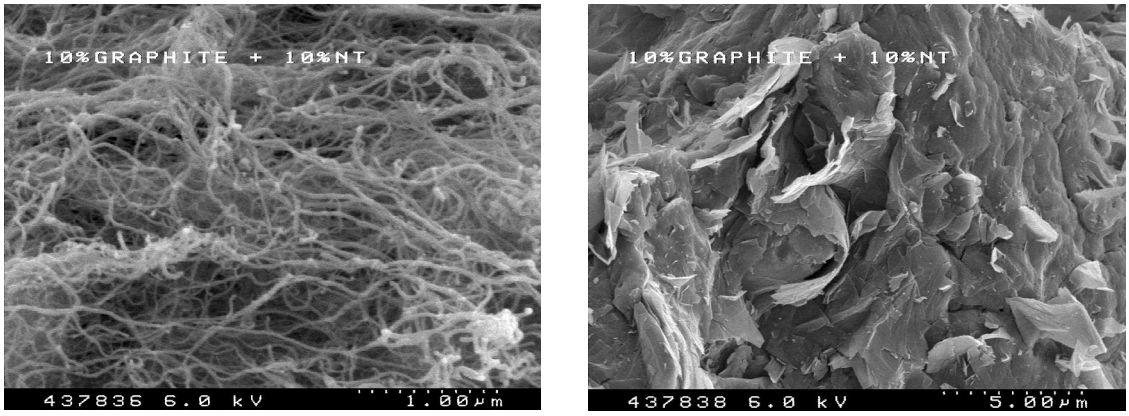

(A) **(B)**

Figure 7-46– SEM images of 10 % nanographite blended with 10 % nanotubes

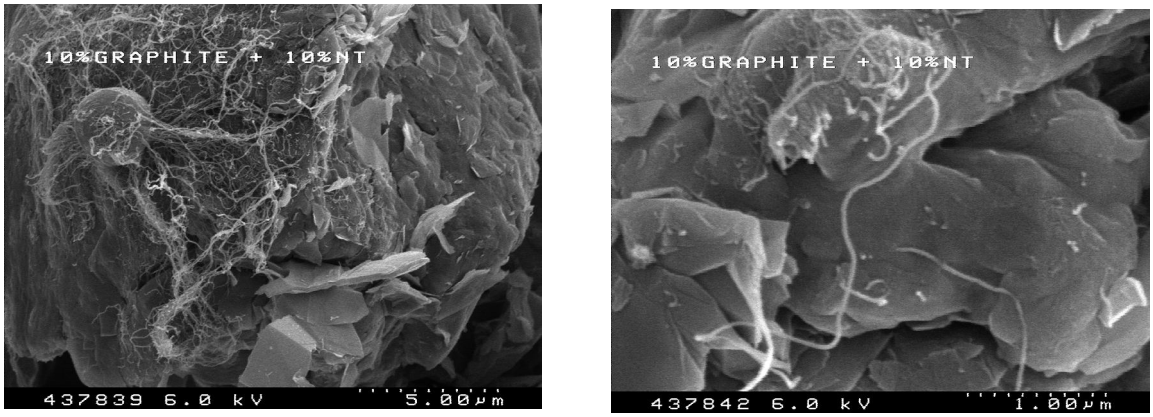

Figure 7-47 - SEM images of 10 % nanographite blended with 10 % nanotubes

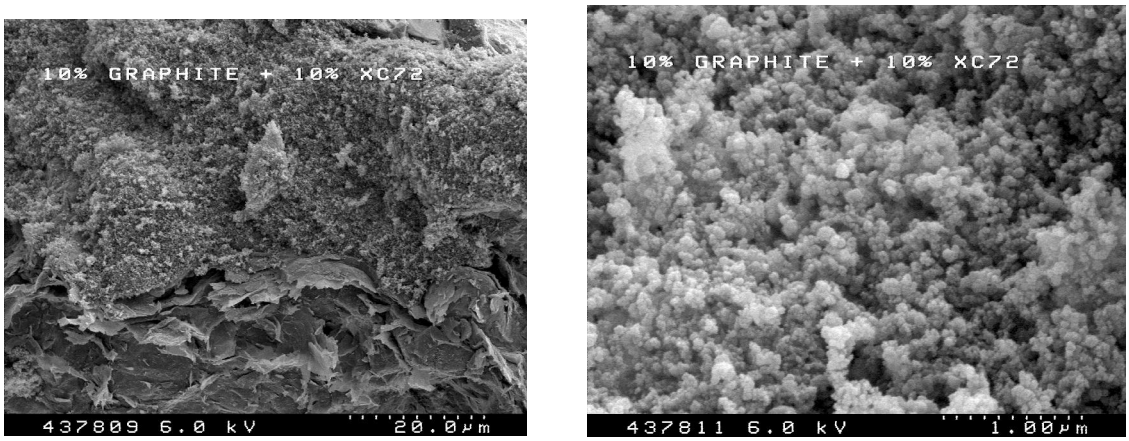

Figure 7-48 – SEM images of 10 % nanographite + 10 % XC72

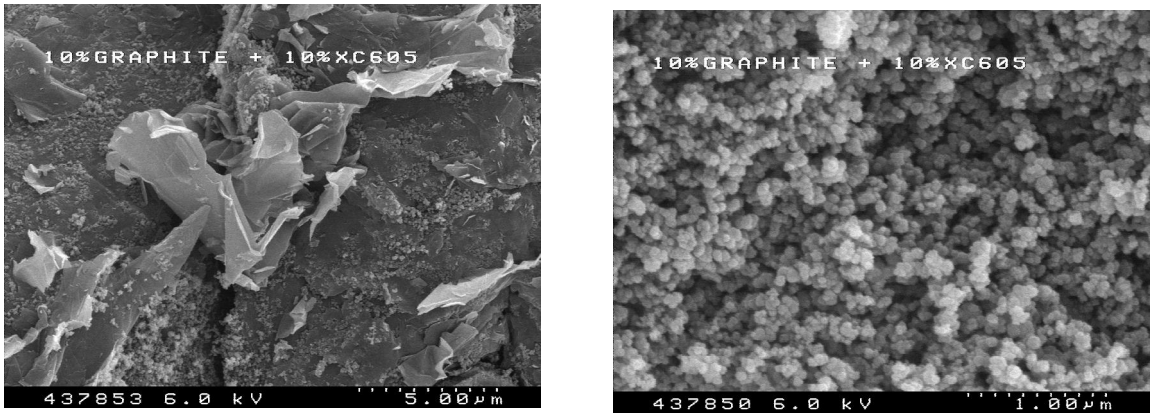

Figure 7-49 – SEM images of 10 % nanographite + 10 % XC605

7-3-3-9 Extrusion

In order to compare direct blending and extrusion in terms of the conductivity of the resultant materials, increasing quantities of nanographite + PES-based co-polymer (10-70 % nanographite) were directly blended before passing through the extruder. The resultant graph can be seen in Figure 7-50.

It can be seen from the graph that the conductivity increases exponentially with increasing graphite concentration, as expected. Both graphs follow the same curve, though the conductivity of the extruded material is always less than that of the directly

blended material. For purposes of comparison, the 40 % blends will be discussed. The directly blended material has a conductivity of 7.2-7.7 x 10^3 S/m compared with a conductivity of 4.0-6.5 S/m for the extruded material at this loading level, which is a difference of 3 orders of magnitude. It can be seen from the graph that this difference is typical and it is therefore stated that the conductivity of the extruded material is significantly less than that of the blended material.

The possibility that a significant amount of carbon was being lost within the extruder was considered, and therefore a sample of 10 % blended nanographite and 10 % extruded nanographite was submitted for microanalysis – results can be seen in Table 7-15. It can be clearly seen that there is no loss of carbon occurring within the extruder and therefore the loss in conductivity must be attributed to morphological effects.

It was decided to put a 10 % nanographite blend through the extruder a total of three times in order to see the effect upon conductivity. The resultant graph can be seen in Figure 7-51. It is seen that the conductivity drops significantly upon exposure to the extruder multiple times, going from 4.0-6.5 S/m in the case of the once extruded material to 4.7-5.2 x 10^{-6} in the case of the material which has been extruded three times. It was noticed that the discs became harder to press as the material became increasingly brittle upon exposure to the extruder on multiple occasions, most likely due to increasing loss of moisture. The fibres could no longer be drawn onto spools. It will be noted from the rheological studies that the melt tended to undergo instability in flow and it is not entirely surprising that problems were encountered in the spinning of the fibres.

It was decided to determine if it was purely the effect of heat exposure which was causing this significant loss of conductivity in the sample. In order to test this theory a pressed disc of 10 % nanographite was exposed to an oven for an hour at 270°C (the temperature of the extruder die). Upon testing, the conductivity was found to have fallen from 5.2 x 10^2 S/m to 1.2-1.4 x 10^2 S/m. After exposure for a further 4 hours, and subsequently overnight, it was seen that the conductivity was maintained at this same level, see Figure 7-52. From this study it is concluded that exposure to heat is affecting

the levels of conductivity that can be achieved with the composite. It may be that the platelet-platelet contacts of the nanographite are being adversely affected, with the extruder introducing an orientational order to the materials, which is having a detrimental affect upon the conductivity.

In order to compare 10 % nanographite discs before, and after, exposure to the oven SEM images of the materials were obtained and can be seen in Figure 7-53 and Figure 7-54. It is seen from these images that the dispersion appears to be better after exposure to the oven, again, suggesting that a better dispersion is having a detrimental affect upon the conductivity, by affecting the percolation pathway and hence the resultant conductivity.

In addition, the effect that the inclusion of carbon nanotubes and carbon black has upon the conductivity of 10 % nanographite after processing in the extruder was also studied. The conductivities can be seen in Table 7-13. It can be seen here that the conductivity is not effectively enhanced in either case. There is a small increase with the addition of 5 % nanotubes – the conductivity moved from 1.5-1.9 x 10^{-1} S/m in the case of the extruded nanographite to 1.9-2.3 x 10^{-1} S/m with the inclusion of the nanotubes. There was a relatively small increase to 2.5-2.7 x 10^{-1} S/m when considering the inclusion of 20 % carbon black

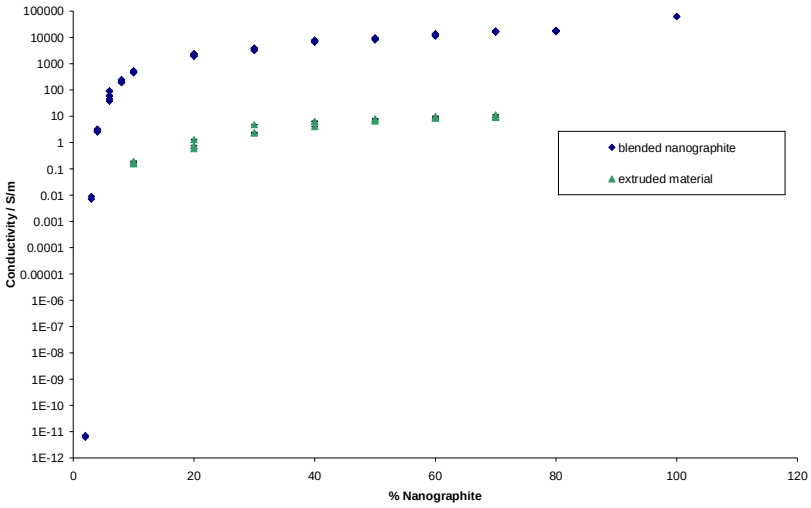

Figure 7-50 – Conductivity comparisons of direct blending and extrusion of increasing concentrations of nanographite

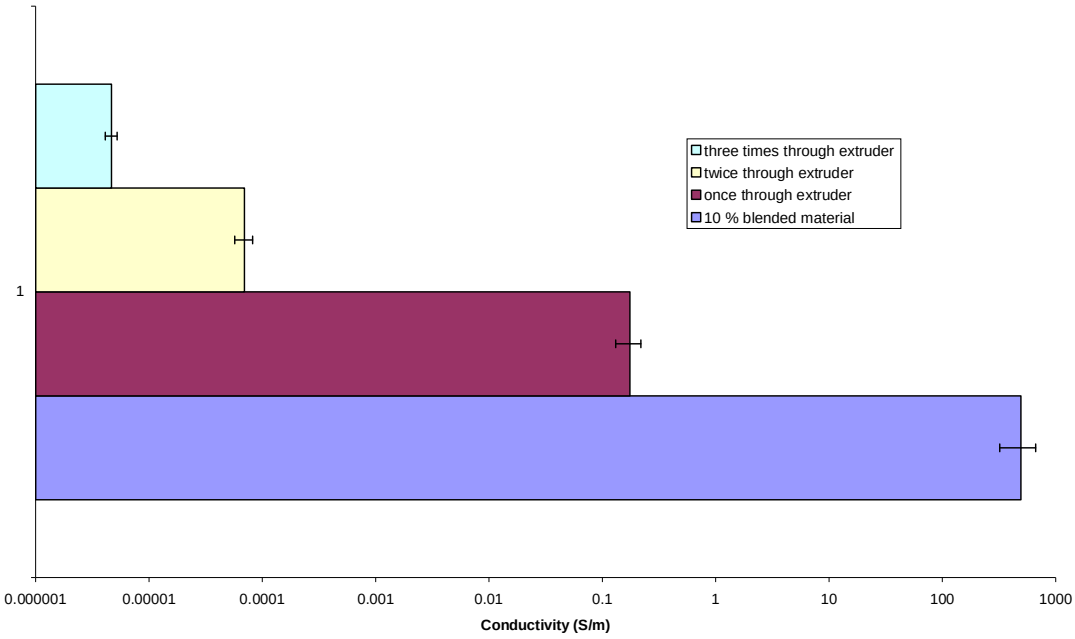

Figure 7-51 – 10 % nanographite through extruder multiple times

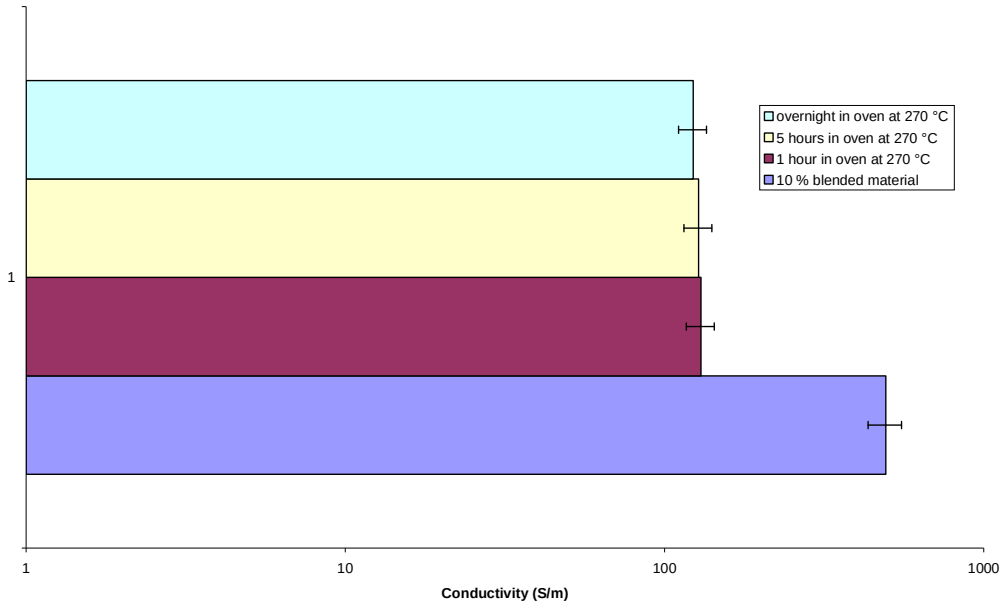

Figure 7-52 – Conductivity comparisons of 10 % nanographite / PES-based co-polymer after exposure to oven over time

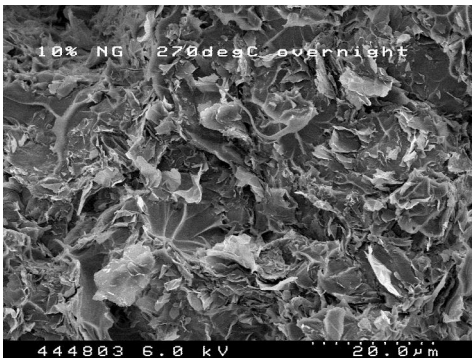

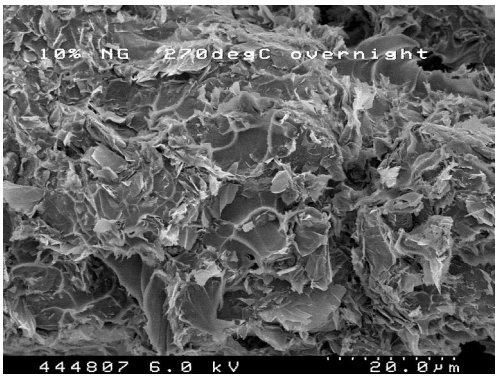

Figure 7-53 –SEM images of 10 % nanographite discs after exposure to oven overnight

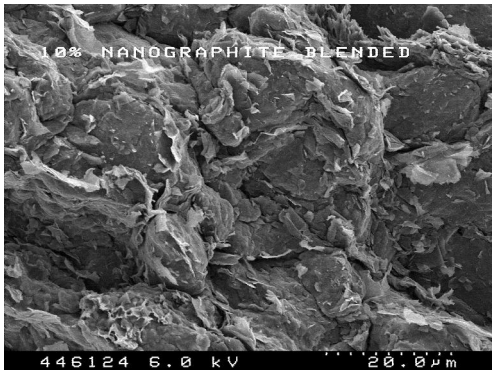

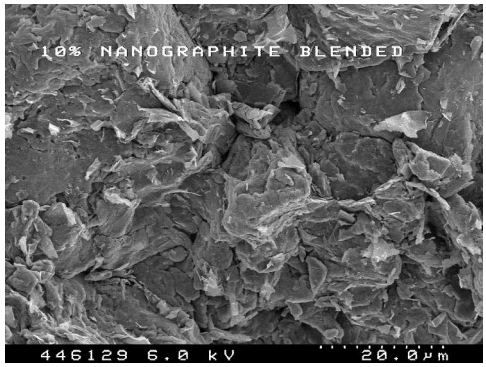

Figure 7-54 SEM images of **10 % nanographite directly blended**

Table 7-13–Conductivities of extruded materials

Material	Conductivity / S/m
10 % nanographite extruded	$1.5 - 1.9 \times 10^{-1}$
10 % nanographite + 5 % nanotubes extruded	$1.9\text{-}2.3 \times 10^{-1}$
10 % nanographite + 20 % XC605 extruded	$2.5\text{-}2.7 \times 10^{-1}$

7-3-3-10 Plasti-Corder®

The conductivity of a blend of 10 % nanographite/PES-based co-polymer after mixing in a Plasti-Corder® was determined, in triplicate, using a four-point probe. The experimental procedure utilised in this study can be seen in Section 6-3-12-2. The results

can be seen in Figure 7-55 and Table 7-14. This conductivity was then compared with the powder blend before processing, and the 10 % nanographite/PES-based co-polymer material which has been processed through the extruder. There was also a comparison with material which had been processed in the Plasti-Corder®, before passing through a twin screw extruder. These results can also be seen in Figure 7-55. It is seen from this Figure that the conductivities have a variation in the region of eight orders of magnitude between the most conductive material (10 % nonographite powder), with a conductivity of 4.5-5.3 x 10^{2} S/m and the least conductive material (the material processed in the Plasti-Corder® before processing through the extruder), with a conductivity of 6.8-7.4 x 10^{-6} S/m.

When one considers 10 % nanographite/PES-based co-polymer blend which has been processed in the extruder, it can be seen that it has a very similar conductivity to the material after processing in the Plasti-Corder®. The conductivity was found to be 1.5-1.9 x 10^{-1} S/cm and 2.4-2.8 x 10^{-1} S/m, respectively. The difference may be due to the fact that the degree of mixing in the Plasti-Corder® was not as efficient as that achieved in the extruder.

After the 10 % nanographite/PES-based co-polymer blend was processed in the Plasti-Corder® it was subsequently processed through the extruder, and the conductivity was found to drop to 6.8-7.4 x 10^{-6} S/cm. This is a drop of over five orders of magnitude. Again, a sample of the material was submitted for microanalysis in order to determine if there is a significant loss of carbon during processing. It can be seen, from Table 7-15, that there is no significant carbon loss and therefore this drop in conductivity is not linked to residual carbon levels.

SEM images of the material which had been processed in the extruder and Plasti-Corder® can be seen in Figure 7-56. These images show a very effective dispersion of the graphite, and this work, again, serves to prove that the application of heat is having an affect upon the morphology of the nanographite which, in turn is lowering the conductivity.

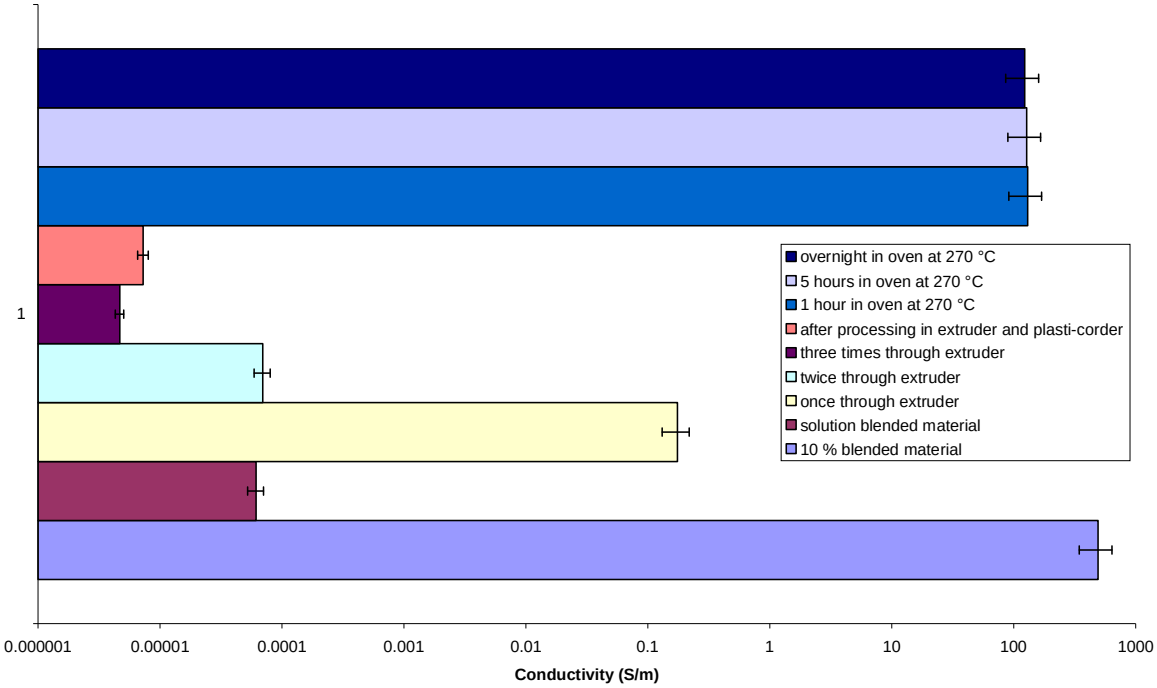

Figure 7-55 – 10 % nanographite conductivity comparison

Table 7-14 – Conductivities of 10 % nanographite materials after processing

10 % Nanographite;	**Conductivity / Sm^{-1}**
powder	$4.5\text{-}5.3 \times 10^{2}$
Solution blended	$4.7\text{-}7.6 \times 10^{-5}$
Processed in extruder once	$1.5\text{-}1.9 \times 10^{-1}$
Processed in extruder twice	$6.5\text{-}8.4 \times 10^{-5}$
Processed in extruder three times	$4.7\text{-}5.1 \times 10^{-6}$
Processed in extruder followed by Plasti-Corder®	$7.1\text{-}7.5 \times 10^{-6}$
Exposed to oven at 270°C for one hour	$1.3\text{-}1.4 \times 10^{2}$
Exposed to oven at 270°C for five hours	$1.2\text{-}1.4 \times 10^{2}$
Exposed to oven at 270°C overnight	$1.1\text{-}1.3 \times 10^{2}$

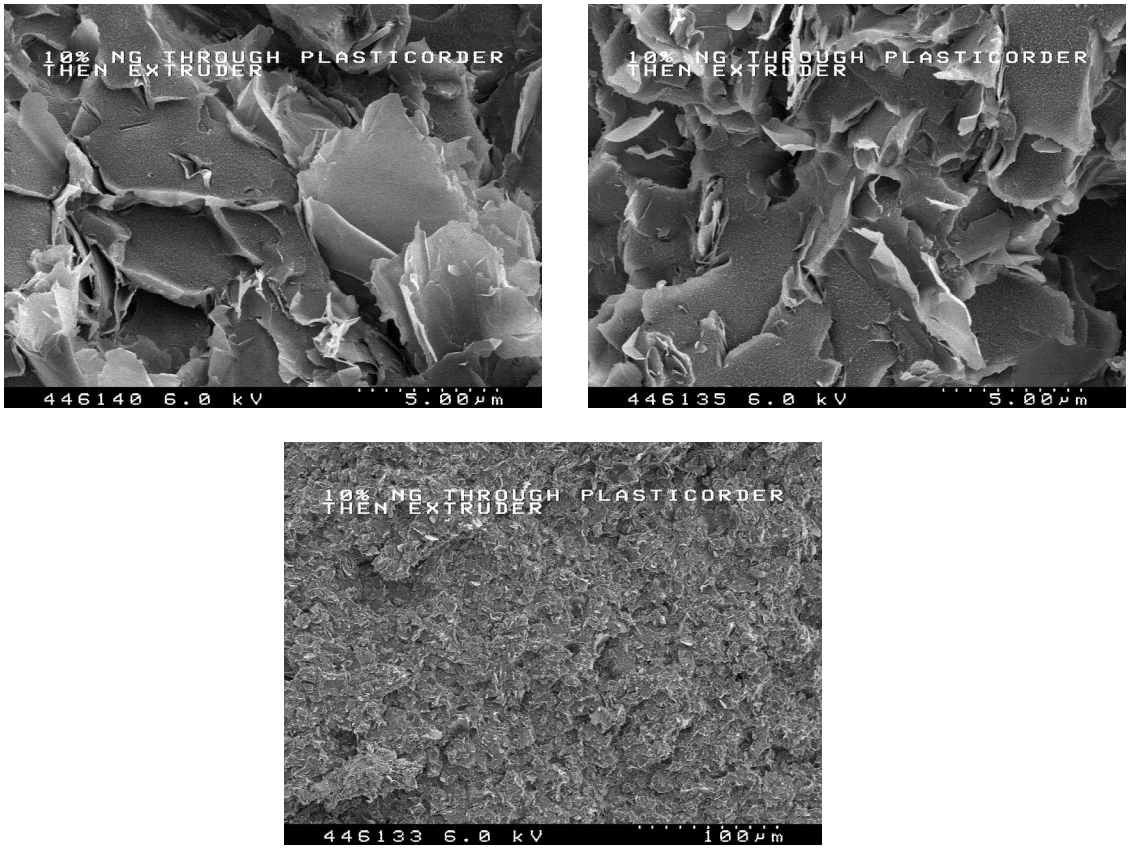

Figure 7-56 – SEM images of 10 % nanographite through extruder and Plasti-Corder®

7-3-3-11 Hot-Stage Microscopy

Hot-stage microscopy was carried out on PES-based co-polymer fibres according to the experimental procedure detailed in Section 6-3-9. In Figure 7-57 the ideal fibre dissolution can be seen. The fibre is composed of PES-based co-polymer, with a thickness of approximately 50 µm. Heated at 3°C per minute up to a temperature of 120°C, it is seen to take just over 30 minutes in order to completely dissolve. It is noted that this fibre was spun by Cytec. In Figure 7-58 and Figure 7-59, the dissolution of a 0.1 % nanographite fibre and 0.4 % nanographite fibres can be seen. It is noted, firstly, that the fibres are much thicker than that of the previously mentioned PES-based co-polymer fibre, with thicknesses of ~300 µm and ~260 µm, respectively. It is also noted

that the fibres were heated for ~2 hours and ~2.3 hours, respectively, and in this time they do not completely dissolve. In comparison, the 0.1 % nanotube fibre and 0.4 % nanotube fibre, seen in Figure 7-60 and Figure 7-61, with thicknesses of ~170 µm and ~200 µm, respectively, do completely dissolve, albeit taking much longer than the idealised PES-based co-polymer fibre. The 0.1 % nanotube fibre dissolves in approximately 1 hour and the 0.4 % nanotube fibre dissolves in approximately 2 hours.

An interesting observation noted when comparing the nanographite fibres to the nanotube fibres is that it is seen that the nanotube fibres appear to contain quite large aggregates of nanomaterial, up to approximately 80 µm in thickness, while the nanographite fibres do not appear to contain large aggregates to the same extent. It is therefore postulated that the better-dispersed nanographite could be acting as a physical barrier to the dissolution of the thermoplastic.

It should be noted, however, that it may actually be advantageous for the thermoplastic fibres containing the nanomaterial not to fully dissolve, leading to the nanomaterial staying in the conductive pathways they achieve while contained in the fibres, see Figure 7-62. It is seen that when the fibres dissolve, the conductive material is carried from the fibre, leading to a possible disruption in the percolation pathway.

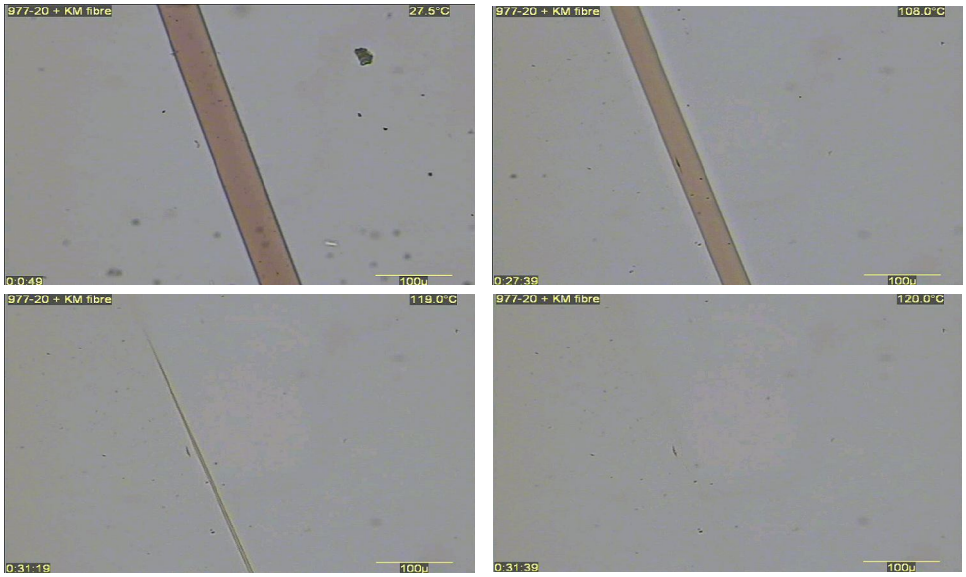

Figure 7-57 – PES-based co-polymer Fibre Dissolution

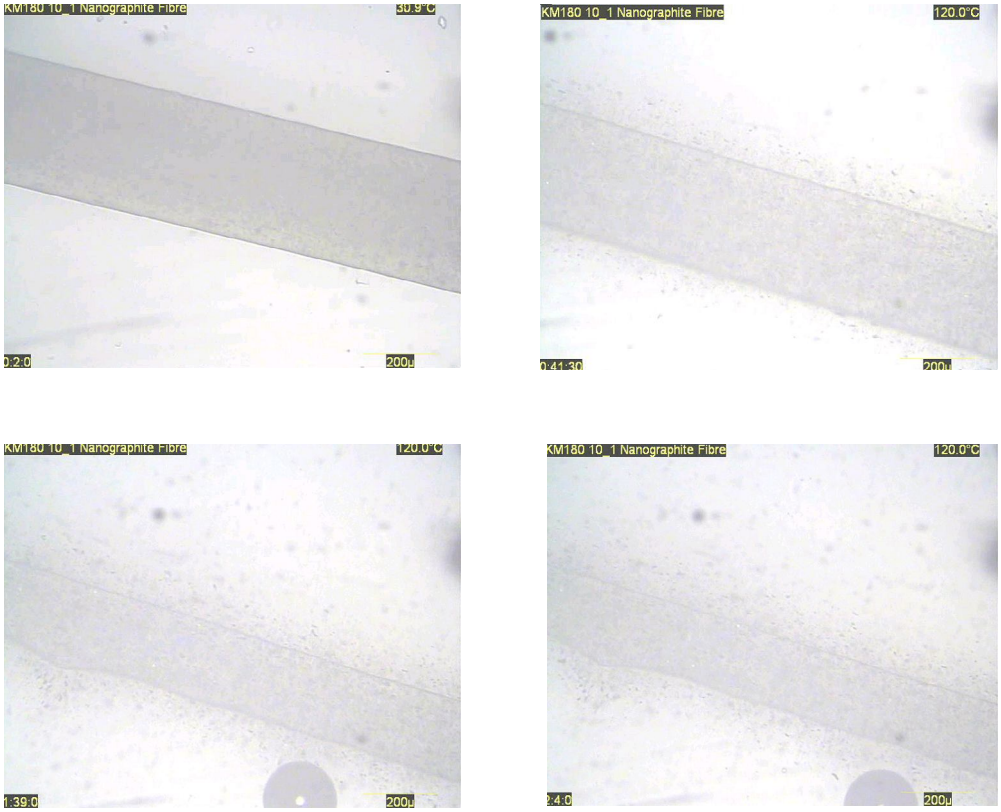

Figure 7-58– 0.1 % Nanographite fibre dissolution

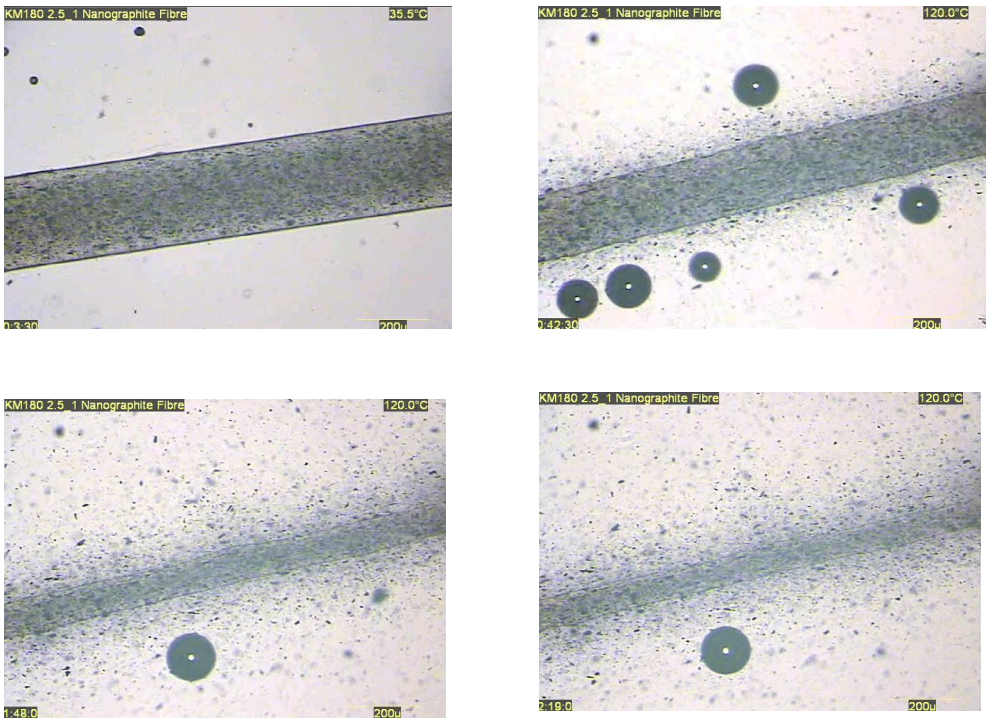

Figure 7-59 - 0.4 % Nanographite fibre dissolution

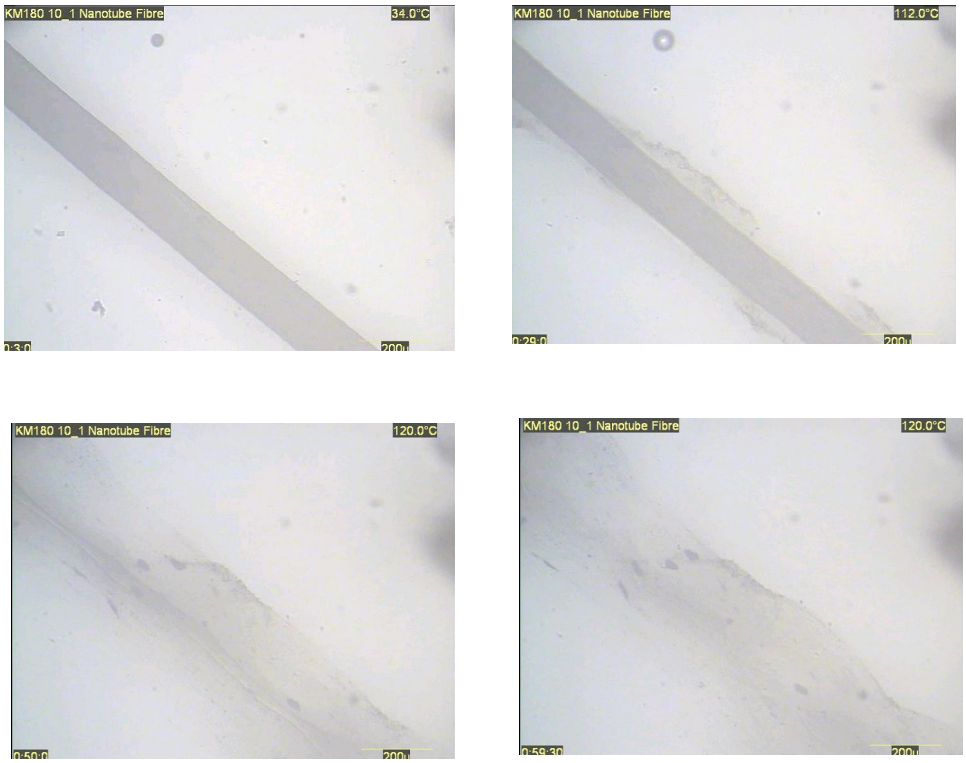

Figure 7-60- 0.1 % Nanotube fibre dissolution

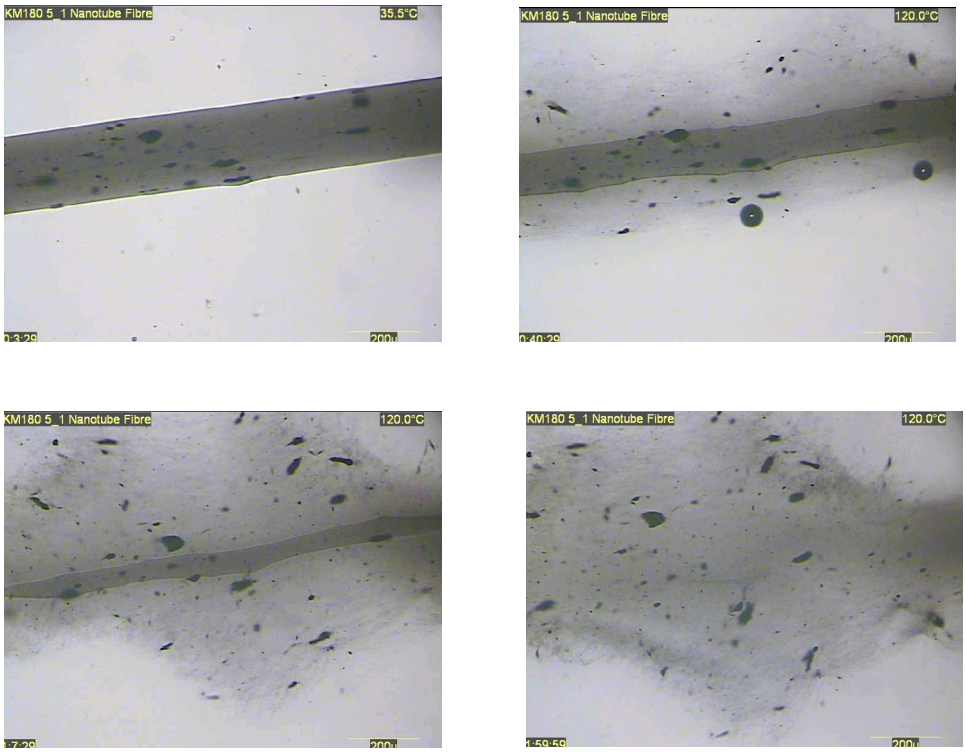

Figure 7-61- 0.4 % Nanotube fibre dissolution

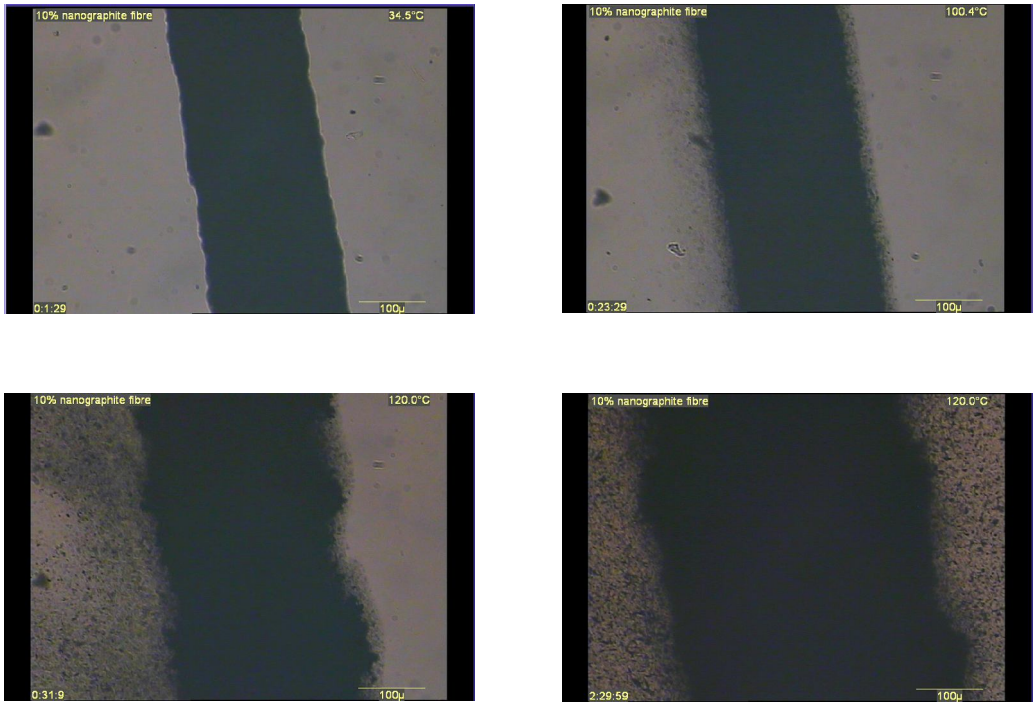

Figure 7-62 10 % Nanographite fibre dissolution

7-3-3-12 Laboratory Scale Melt-Spinning

The PES-based co-polymer was processed in a heated spinning block according to the procedure detailed in Section 6-3-13. It was found that fibres of a very similar nature to those formed in the extruder were readily generated. Unfortunately, when 10 % nanographite was introduced into the powder blend, the processability of the instrument was compromised, and the molten polymer blend would no longer be forced through the die, even with a high nitrogen flow. It was concluded that the viscosity of the nanographite was too high that this method of polymer processing could no longer be utilised effectively.

7-3-3-13 PEEK and PEKK

In order to determine how the nanographite behaves when introduced into alternative engineering thermoplastics, it was decided to study the direct blending with PEEK and

PEKK, by the same method as that outlined for blending PES-based co-polymer, see Section 6-3-10-2-1. As both of these materials were initially very coarse, intensive ball milling over a period of approximately 12 hours was required in order to create the fine powder required.

The resultant graphs, displayed in Figure 7-63 and Figure 7-64 show that the conductivity is increasing exponentially with increasing nanographite content. For purposes of comparison, included is a chart showing the behaviour of the nanographite when blended with all engineering thermoplastics utilised in this project, see Figure 7-65. It can be seen from this graph, that at the lower concentration of nanographite (up to 50 % wt) there is considerable disparity between the highest level of conductivity and the lowest. For example, when one considers the conductivities of the 30 % blends, detailed in Table 7-12, it can be seen that the PEEK samples have a much higher conductivity of $9.0 \times 10^3 - 1.1 \times 10^4$ S/m, with PES-based co-polymer blends having the lowest conductivity of $3.4\text{-}3.8 \times 10^3$ S/m. At the higher nanographite loadings (>60 %), see Table 7-13, the conductivity of the PEEK/PEKK blends are very similar, having values of $3.6\text{-}4.0 \times 10^4$ and $3.3\text{-}3.9 \times 10^4$ S/m, respectively. This is in comparison with PES-based co-polymer which has a value of $1.8\text{-}1.9 \times 10^4$ S/m for the same loading level.

In order to determine if the differences in conductivity are due to intrinsic differences between the polymers i.e. due to the flow of ions within the lattice, a dielectric frequency sweep was carried out on hot-pressed polymer samples, in a frequency range of 0-60,000 Hz, see Figure 7-66. It can be seen that the highest conductivity is achieved in the case of the PES-based co-polymer sample, which leads to the conclusion that it is not the intrinsic value of conductivity which is responsible for the increased conductivity in the case of the PEEK and PEKK samples.

The densities of the materials can be seen in Table 7-14. A material's density reflects its void structure and its degree of crystallinity – although it does not correlate directly to the available volume, as this is attributable to a combination of both order and disorder within the structure. One, therefore, may expect that the presence of crystallites in the

PEEK and the PEKK material may create a more tortuous pathway for the nanographite material to negotiate, therefore leading to lower conductivity levels.

It can be seen that PEKK has the lowest density, of 1.22 g/cm^{-3} and PEEK has the highest density, of 1.37 g/cm^{-3}. As these are the most conductive materials the density levels cannot be wholly responsible for the conductivity levels reported.

Another factor which could affect the conductivity is moisture levels; the amine end groups of the PES-based co-polymer may become quaternised by exposure to water. This could lead to the liberation of an OH group which could migrate, therefore becoming a charge carrier. As this would effectively lead to an increase in the conductivity level, again, this cannot be the sole cause of the reported conductivities.

The variation in conductivities may simply be attributable to residual catalyst(s) left over from the polymerisation. When PES-based co-polymer is synthesised, bisphenol S is used with potassium carbonate to generate O^- groups. It is possible that this bisphenol has impurities present, potentially in the form of KCl or Cl^-; as there are difficulties involved in the purification of all raw materials utilised, these impurities could be carried over into the final polymer thus affecting the resultant conductivities.

It is therefore concluded that morphological changes which occur within a material as more nanographite is introduced into the system are directly responsible for differences in conductivity. For example, increasing quantities of nanographite has a morphological effect upon the spherulites when introduced into PEEK (discussed in Chapter 3). The difference in conductivities between materials has not been so easy to resolve. As the differences do not appear to be related to mechanical differences between the materials, they have been attributed to the presence of ionic impurities.

Table 7-12 – Conductivities at 30 % nanographite loadings

Sample	Conductivity / Sm^{-1}
PEEK + 30 % Nanographite	9.0×10^{3} -1.1×10^{4}
PEKK + 30 % Nanographite	$5.9\text{-}6.4 \times 10^{3}$
PES-based co-polymer + 30 % Nanographite	$3.4\text{-}3.8 \times 10^{3}$

Table 7-13 – Conductivities at 80 % nanographite loadings

Sample	Conductivity / Sm^{-1}
PEEK + 80 % Nanographite	$3.6\text{-}4.0 \times 10^{4}$
PEKK + 80 % Nanographite	$3.3\text{-}3.9 \times 10^{4}$
PES-based co-polymer + 80 % Nanographite	$1.8\text{-}1.9 \times 10^{4}$

Table 7-14 – Density comparisons

Polymer	Density / gcm^{-3}
PES-based co-polymer	1.35
PEEK	1.37
PEKK	1.22

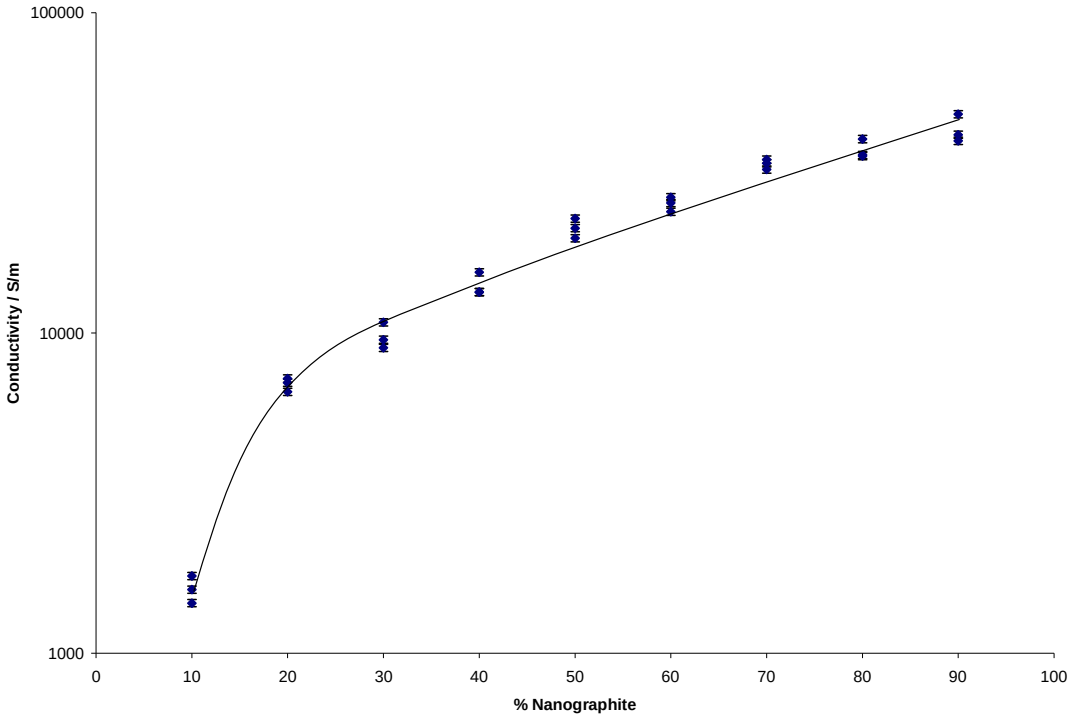

Figure 7-63 – Nanographite directly blended with PEEK

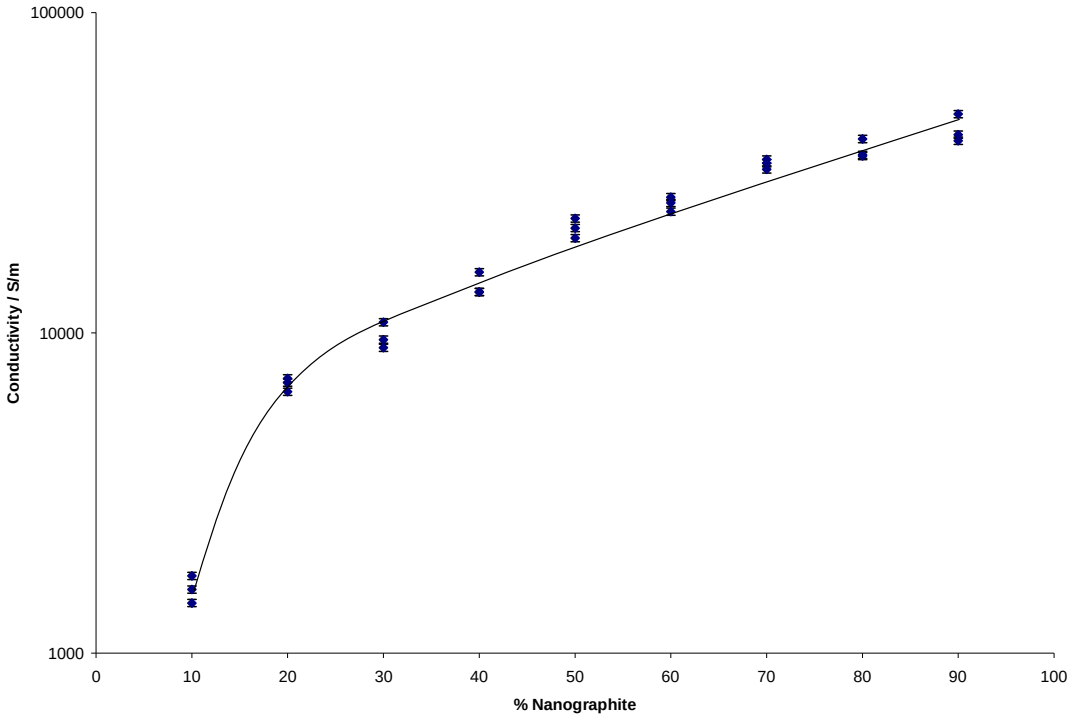

Figure 7-64 – Nanographite directly blended with PEKK

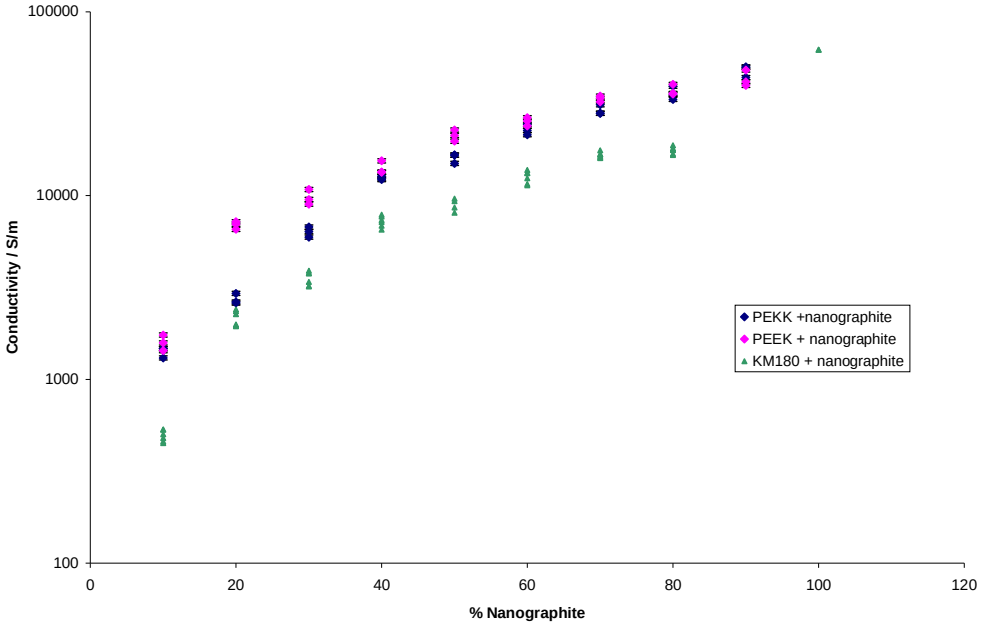

Figure 7-65 – Increasing quantities of nanographite blended with all engineering thermoplastics

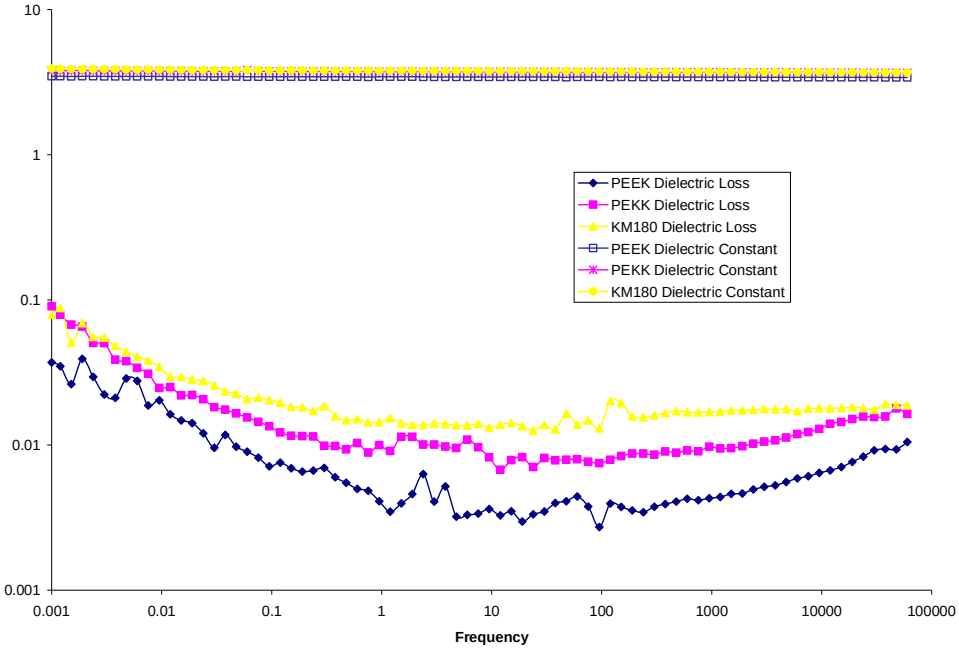

Figure 7-66 – Comparison of dielectric loss and dielectric constant vs. frequency of polymers

7-3-3-14 % Carbon Present

The % carbon, as well as % H, % N and % S present in various materials used, and produced, in this study were measured by microanalysis; the results are shown in Table 7-15. An additional column showing the theoretical % of carbon which would be expected if you were to take powder blends of the included materials is also shown. In addition, a column showing how this theoretical % varies with the actual % carbon present is also included.

It is seen from this table that the % C present does not significantly change depending upon how the material is processed, nor indeed whether it is in powder form. Therefore, as previously discussed, the theory that there is a significant loss of carbon material through extrusion or other processing is disproved. Typically, percentage differences in the region of 1 %, or less, are reported. Though the largest % difference must be commented upon; it was found in the case of 40 % nanographite/60 % PES-based co-polymer extruded fibre – it was 4.54 % less than was theoretically expected. This is most probably due to sampling errors, where a non representative sample was submitted for microanalysis. As this technique only requires samples on the milligram scale, it may be that the small sample submitted for analysis may not have been representative of the bulk of the material.

Table 7-15– Microanalysis results

	% C	% C theoretical	% difference	% H	% N	% S
Nanographite powder	100	-	-	0	0	0
PES-based co-polymer powder	64.35	-	-	2.95	0.66	10.88
PES-based co-polymer fibre	64.39	64.35	+0.06	3.36	0.48	11.64
Nanotube powder	96.87	-	-	0	0	0
10 % ng + 5 % nanotubes extruded	68.95	69.54	-0.85	3.04	0.27	na
XC605 powder	98.36	-	-	0.14	0.11	na
10 % ng* powder	68.02	67.92	+0.15	3.04	0.47	11.13
10 % ng* *in- situ*						
10 % ng* through extruder	68.77	67.92	+1.15	3.14	0	10.60
10 % ng* through plasticorder	67.82	67.92	-0.15	3.21	0.87	10.83
10 % ng* through extruder + plasticorder	67.14	67.92	-1.15	3.27	0.46	11.56
20 % ng* powder	68.48	71.48	-4.29	3.22	0.59	9.73
20 % ng* extruded	70.37	71.48	-1.56	3.17	0.53	9.43
30 % ng* powder	75.46	75.05	+0.54	2.38	0.36	8.67
30 % ng* extruded	74.77	75.05	-0.37	2.98	0.46	10.31
40 % ng* powder	76.76	78.61	-2.38	2.01	0.43	6.91
40% ng* extruded	75.12	78.61	-4.54	2.41	0.45	7.53
10 % ng* + 20 % XC605 powder	72.67	74.72	-2.78	1.97	0.41	na
10 % ng* + 20 % XC605 extruded	74.16	74.72	-0.75	2.26	0.27	8.29

*ng=nanographite *na = not available

7-3-3-15 Specific Gravity Measurements

7-3-3-15-1 Density

The density of various samples was measured by following the experimental procedure and calculations detailed in Section 6-3-17-2. The results are shown in Table 7-16. It is noted that values quoted are an average of three experimental results. It can be seen from the table that the density of the pure nanographite was found to be 2.22 g/cm. This is within the typical density limits of graphite which are 2.2-2.3 g/cm.[8]

It can be seen that the density of PES-based co-polymer in disc form and fibre form was 1.35 g/cm^{-3} and 1.34 g/cm^{-3} respectively, which is in good agreement with published density values of poly(ethersulfone), which are typically 1.37 g/cm^{-3}. As stated, in fibre form the density of the PES-based co-polymer is slightly less, with a value of 1.34 g/cm^{-3}, this slight reduction is most likely due to the presence of void space. The samples of 10 % nanographite in disc form, fibre form and fibre form pressed into a disc were found to be 1.44, 1.41 and 1.41 g/cm^{-3} respectively. The values are, again, not only in good agreement with each other, but are also very similar to the expected density value of 1.44 g/cm^{-3}. The slightly lower values are most likely due to the presence of void space within the sample.

The small drop in density level when comparing the pressed disc and the extruded sample suggests that there is not a significant drop in carbon levels upon processing. When one considers the 10 % nanographite which has been processed in both the extruder and Plasti-Corder® the density was found to be 1.22 g/cm^{-3}, which is significantly lower than anticipated and suggests the presence of significant void space within the disc.

Table 7-16 – Density measurement results

Sample	Density g/cm^{-3}	Expected Density using calculated values
PES-based co-polymer disc	1.35	-
Pure nanographite disc	2.22	-
PES-based co-polymer + 10 % nanographite disc	1.44	1.44
PES-based co-polymer fibre	1.34	1.35
PES-based co-polymer + 10 % nanographite fibre	1.41	1.44
PES-based co-polymer + 10 % nanographite fibre pressed into disc	1.41	1.44
PES-based co-polymer + 10 % nanographite processed in plasticorder and extruder	1.22	1.44

7-4 Conclusions

As discussed at the start of this chapter, the main objective of this project was to explore the potential conductivity benefits which can be achieved through the use of carbon nanographite, and other related fillers, to improve the performance of thermoplastic toughened composite matrix materials.

Initially, the conductivity of a simple polypyrrole and carbon fibre system was investigated. Polypyrrole was synthesised in house as well as purchased from Aldrich and BASF. It was found that the synthesised material had the highest conductivity, in the order of 873-1183 S/m. After doping in acid (HCl and HNO_3), the conductivity was raised as high as 5438 S/m (after exposure to 6M HCl). Again, the synthesised material was found to have the highest conductivity associated. The conductivity of untreated carbon fibre was found to be 696-969 S/m. After doping in a similar fashion to the polypyrrole, the highest conductivity was found to be 14612 S/m (after exposure to 3M HNO_3). The rationale associated with these results is that HCl causes protonation of the nitrogen. A higher conductivity was found for HCl in the case of polypyrrole, as the material is sensitive to oxidation – therefore treatment in HNO_3 leads to cleavage of the double bonds causing a loss in conjugation. In comparison, doping carbon fibre in HNO_3 led to the highest associated conductivity. This was linked to topographical reasons, with increased surface roughness leading to increased acidic functions in this case.

Moving on to the nanomaterial-containing systems, a comparison study was undertaken to determine the conductivity associated with PES-based co-polymer/nanographite samples after solution blending, *in-situ* processing and direct blending. It was seen that the conductivity of 10 % nanographite processed *in situ* was found to be very low, in the order of 7.4×10^{-12} S/m. In comparison, solution blending was found to produce composites which percolate at approximately 8 %, with the highest conductivity associated with the 80 % loading level – $7.4\text{-}9.2 \times 10^{2}$ S/m. The directly blended material was found to produce powders which percolated at approximately 3 %, with the highest conductivity associated with the 80 % loading level – 1×10^{4} S/m.

This large disparity has been attributed to the level of dispersion achieved in each case. In the case of the *in-situ* produced materials, a very effective dispersion of the nanomaterial was produced. This led to the introduction of polymer particles between the nanographite platelets, causing a disruption in the percolation pathway, and therefore a loss in the resultant conductivity. Again a reasonable dispersion was found when carrying out solution blending work. In addition, chloroform was used as a solvent for this work, and chloroform was found to become trapped within the pores of the composites, again, causing a disruption of the percolation pathway. When one considers the directly blended materials, there was no interference with the platelet-platelet contacts, and subsequently the conductivity was found to be much higher in this case.

In order to further enhance the conductivity of 10 % nanographite blended with PES-based co-polymer, increasing quantities of carbon nanotubes, carbon black and phthalocyanine were included. In the case of the carbon nanotubes it was seen that a small enhancement in the conductivity was seen with the addition of up to 10 wt% nanotubes. This small enhancement was attributed to the materials coming together in an enhancive manner, with the nanotubes acting as mini-wires connecting together the graphite platelets.

The carbon black and the phthalocyanine did not effectively enhance the conductivity of the matrix. From SEM images the carbon black was seen to exist discretely within the matrix. As this material is spherical in shape the aspect ratio is lower than the graphite platelets and as a result there was no enhancement effect observed. Regarding the phthalocyanine, it was observed that additional doping may be required in order for it to be an effective material.

An extruder was also utilised to determine how conductive processed materials could be. It was seen that, for the same wt% of nanographite, the conductivities of extruded material were approximately three orders of magnitude less than the blended materials. Again, this was attributed to the effective dispersion and orientation gained in the instrument leading to a loss in conductivity. Subsequent additions of carbon nanotubes and carbon black failed to enhance the conductivity to a large extent.

Further studies using a Plasti-Corder® and an oven also confirmed that the application of heat was aiding dispersion of the nanographite and causing subsequent loss in the conductivities possible.

Nanographite was blended with other engineering thermoplastics – namely PEEK and PEKK. It was found that both materials led to a higher conductivity than the PES-based co-polymer. The differences were not linked to any physical reasons and were therefore attributable to the presence of ionic impurities within the matrix leading to a higher than expected conductivity.

Interestingly, it was seen that additions of TTF TCNQ were found to rebuild the percolation pathway, by the growing of long needle-like crystals using a slow cooling technique. The conductivities achieved were not of the level of the directly blended material but they do serve to prove that it is possible to rebuild a percolation pathway which has been reduced.

7-5 References

1. B. Sun, J.J. Jones, R.P. Furford, M. Skyllas-Kazacos, *Stability and Mechanical Properties of Electrochemically Prepared Conducting Polypyrrole Films.* Journal of Materials Science, 1989. **24**: p. 4024.

2. L.B. Nohara, G.P. Filho, E.L. Nohara, M.U. Kleine, M.C. Rezende, *Evaluation of Carbon Fibre Surface Treated by Chemical and Cold Plasma Processes.* Materials Research, 2005. **8**(3): p. 281-286.

3. M. Kilbride, R.A. Pethrick, S. Ward, M. Harriman, *Influence of Nanographite and Other Nanofillers on the Properties of Thermoset: Thermoplastic Blends for Composite Matrices.* Materials Research Society Fall Meeting, Boston, USA, 2007.

4. G. Grimwall, *Thermophysical Properties of Materials*. 1999, North Holland

5. S. Arslan, I. Yilmaz, *Preparation, electrochemical, and spectroelectrochemical characterization of a new water-soluble copper phthalocyanine.* Inorganic Chemistry Communications, 2006. **10**: p. 385-388.

6. B.N. Achar, P.K. Jayasree, *New "molecular metals" based on symmetrical tetrasubstituted copper phthalocyanine complexes.* Canadian Journal of Chemistry, 1999. **77**(10): p. 1690-1696.

7. J.R. Andersen, E.M. Engler, K. Bechgaard, *Organic Growth: Basic Crystal-Growth Techniques.* Annals New York Academy of Sciences, Part II. Organic Materials, 1977. **313**: p. 293-300.

8. Asbury Carbon *technical data sheet on natural graphite*

Appendix 1 – Correction factors used in four-point probe

C.F.$_1$(d/s)	Circle	Square	Rectangle L/W=2	Rectangle L/W=3	Rectangle L/W=4
1.0				0.9988	0.9994
1.25				1.2467	1.2248
1.5			1.4788	1.4893	1.4893
1.75			1.7196	1.7238	1.7238
2.0			1.9475	1.9475	1.9475
2.5			2.3532	2.3541	2.3541
3.0	2.2662	2.4575	2.7000	2.7005	2.7005
4.0	2.9289	3.1127	3.2246	3.2248	3.2248
5.0	3.3625	3.5098	3.5749	3.5750	3.5750
7.5	3.9273	4.0095	4.0361	4.0362	4.0362
10.0	4.1716	4.2209	4.2357	4.2357	4.2357
15.0	4.3646	4.3882	4.3947	4.3947	4.3947
20.0	4.4364	4.4516	4.4553	4.4553	4.4553
32.0	4.4791	4.4878	4.4899	4.4899	4.4899
40.0	4.5076	4.5120	4.5129	4.5129	4.5129
infinity	4.5324	4.5324	4.5325	4.5325	4.5324

C.F.$_2$(t/s)	F (t/s)
< 0.4	1.000
0.400	0.9995
0.500	0.9974
0.555	0.9948
0.625	0.9896
0.714	0.9798
0.833	0.9600
1.000	0.9214
1.111	0.8907
1.250	0.8490
1.429	0.7938
1.667	0.7225
2.000	0.6336

Appendix 2 – Error calculations

Part 1 - Error calculations used for polypyrrole conductivity calculations.

It is subsequently assumed that the error calculated is applicable to all four-point probe measurements within each sample type

$$\sigma = \frac{I}{t \times V \times CF} = \frac{1}{t \times R \times CF_1}$$

The error associated with the conductivity is therefore calculated as being the sum of errors on resistance *R*, thickness *t* and correction factor CF_1:

$$\frac{d\sigma}{\sigma} = \frac{dR}{R} + \frac{dt}{t} + \frac{dCF}{CF}$$

Sample type	**Thickness (x 10^{-4}m)**	***dt* (x10^{-6} m)**	**(*dt* / *t*) max**	**Resistance (Ω)**	***dR* (Ω)**	**(*dR* / *R*) max**	**$d\sigma / \sigma$ (%)**
Aldrich discs	5.23-5.61	10	0.0191	4.12-6.14	0.01	0.0024	2.2
BASF films	0.6-0.62	1	0.0167	9.7-12.1	0.01	0.00103	2.6
Synthesised films	0.40-0.44	1	0.0250	5.1-7.6	0.01	0.00196	2.7

Part 2 - Error calculations used for carbon fibre conductivity calculations.

$$\sigma = \frac{1}{R} \times \frac{l}{A}$$

The error associated with the conductivity will therefore be equal to the sum of the errors on the resistance *R*, thickness *t* and twice the error associated with the diameter *D*:

$$\frac{d\sigma}{\sigma} = \frac{dR}{R} + \frac{dl}{l} + 2 \times \frac{dD}{D}$$

It is subsequently assumed that this calculated error is applicable to all carbon fibre samples

	Diameter (x 10^{-5}m)	dD (x 10^{-6}m)	(dD / d) max	Length (x 10^{-3}m)	dl	(dl / l) max	Resistance(Ω)	dR	(dR / R) max	$d\sigma$ / σ (%)
Undoped carbon fibre	6-8	1	0.016	4.1-7.0	0.0001	0.024	1500-2000	10	0.0067	6.3

Part 3 - Error calculations used for nanographite

Error calculated using a sample of 10 % nanographite

Measurement number	Thickness (x 10^{-4}m)	dt (x10^{-6} m)	(dt / t) max	Resistance (Ω)	dR (Ω)	(dR / R)	$d\sigma$ / σ (%)
1	7.17	10	0.0139	0.806	0.01	0.0124	2.6
2	7.17	10	0.0139	0.822	0.01	0.0122	2.6
3	7.17	10	0.0139	0.815	0.01	0.0123	2.6
4	7.17	10	0.0139	0.791	0.01	0.0126	2.7
5	7.17	10	0.0139	0.796	0.01	0.0126	2.7
6	7.17	10	0.0139	0.801	0.01	0.0125	2.6
7	7.17	10	0.0139	0.808	0.01	0.0124	2.6
8	7.17	10	0.0139	0.806	0.01	0.0124	2.6
9	7.17	10	0.0139	0.798	0.01	0.0125	2.6
10	7.17	10	0.0139	0.791	0.01	0.0126	2.7

Average error = 2.6